



Dear Author:

Thank you for publishing with AGU. Your proofs are attached. AGU and Wiley are committed to rapid posting of accepted papers. The accepted version of your paper is already available online (except for embargoed papers), providing visibility, and we strive to have final versions available within a few weeks. Following the guidelines for marking corrections and returning the proofs quickly will allow prompt online posting of the final version of your paper.

AGU Publications recently [updated](#) our style to follow leading practices in scholarly publishing, to simplify corrections and reduce copyediting changes. We are now following the APA style for grammar and markup. This style is used by many other journals and we hope that this change, over time, will lead to a simpler and standard experience for authors.

We have collected some information on how to increase the visibility of your paper [here](#). Many of these steps can be taken after publication, so it is not too late to start. The online version of your paper includes “Altmetrics,” which continually tracks and links to mentions in news outlets, Twitter, blogs, and other social media. A link to articles that cite your paper is also provided. Papers are also linked directly to any highlights provided by AGU and other similar AGU content. Recent highlights across AGU journals are collected [here](#).

AGU is also, through Wiley, working to expand sharing of articles. Wiley piloted an [initiative](#) through the PDF reader Readcube that allows content to be shared freely to colleagues by authors and subscribers. This is now available for AGU content. For authors and subscribers, just click on the “share” link of your article in the Readcube reader. For the public and general reader, this service also allows free access to Wiley and thus AGU content from links in news stories.

Finally, your feedback is important to us. If you have questions or comments regarding your AGU Publications experience, including information on production and proofs, please contact us at [publications@agu.org](mailto:publications@agu.org). We will also be contacting you soon after your article is published with an author survey. Please take a few minutes to respond to this online survey; your input is important in improving the overall editorial and production process. Thank you again for supporting AGU.

Sincerely,

Brooks Hanson  
Sr. Vice President, Publications

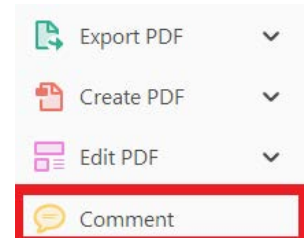
## USING e-ANNOTATION TOOLS FOR ELECTRONIC PROOF CORRECTION

**Required software to e-Annotate PDFs: Adobe Acrobat Professional or Adobe Reader (version 11 or above). (Note that this document uses screenshots from Adobe Reader DC.)**

The latest version of Acrobat Reader can be downloaded for free at: <http://get.adobe.com/reader/>

Once you have Acrobat Reader open on your computer, click on the **Comment** tab (right-hand panel or under the Tools menu).

This will open up a ribbon panel at the top of the document. Using a tool will place a comment in the right-hand panel. The tools you will use for annotating your proof are shown below:



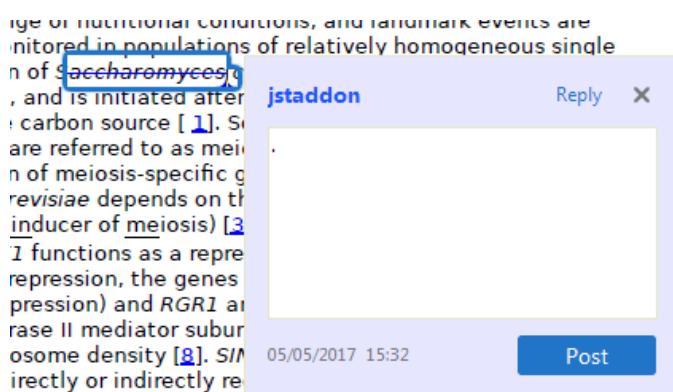
### 1. Replace (Ins) Tool – for replacing text.



Strikes a line through text and opens up a text box where replacement text can be entered.

#### How to use it:

- Highlight a word or sentence.
- Click on .
- Type the replacement text into the blue box that appears.



### 2. Strikethrough (Del) Tool – for deleting text.



Strikes a red line through text that is to be deleted.

#### How to use it:

- Highlight a word or sentence.
- Click on .
- The text will be struck out in red.

experimental data if available. For ORFs to be had to meet all of the following criteria:

- Small size (35–250 amino acids).
- Absence of similarity to known proteins.
- Absence of functional data which could indicate the real overlapping gene.
- Greater than 25% overlap at the N-terminal terminus with another coding feature; over both ends; or ORF containing a tRNA.

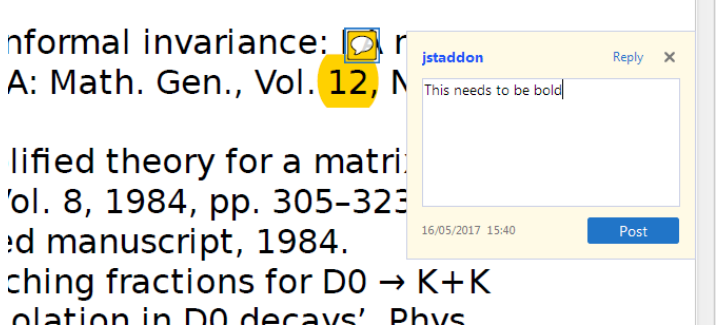
### 3. Commenting Tool – for highlighting a section to be changed to bold or italic or for general comments.



Use these 2 tools to highlight the text where a comment is then made.

#### How to use it:

- Click on .
- Click and drag over the text you need to highlight for the comment you will add.
- Click on .
- Click close to the text you just highlighted.
- Type any instructions regarding the text to be altered into the box that appears.



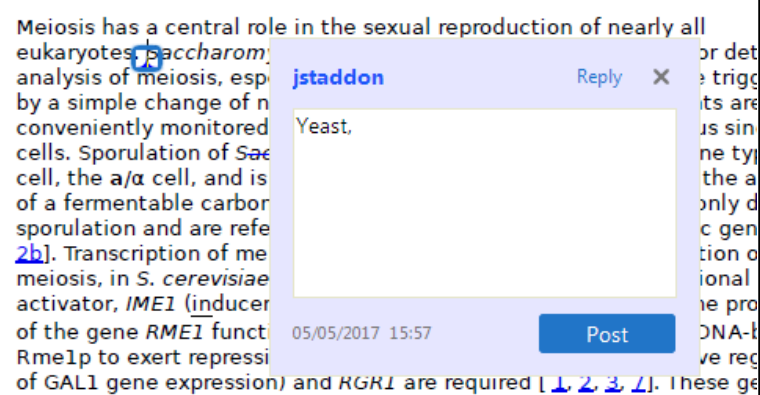
### 4. Insert Tool – for inserting missing text at specific points in the text.



Marks an insertion point in the text and opens up a text box where comments can be entered.

#### How to use it:

- Click on .
- Click at the point in the proof where the comment should be inserted.
- Type the comment into the box that appears.



**5. Attach File Tool – for inserting large amounts of text or replacement figures.**



Inserts an icon linking to the attached file in the appropriate place in the text.

**How to use it:**

- Click on .
- Click on the proof to where you'd like the attached file to be linked.
- Select the file to be attached from your computer or network.
- Select the colour and type of icon that will appear in the proof. Click OK.

The attachment appears in the right-hand panel.

chondrial preparation  
ative damage injury  
e extent of membra  
l, malondialdehyde (TBARS) formation. I  
used by high perform

**6. Add stamp Tool – for approving a proof if no corrections are required.**



Inserts a selected stamp onto an appropriate place in the proof.

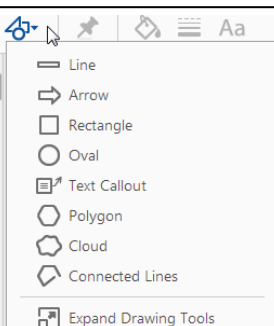
**How to use it:**

- Click on .
- Select the stamp you want to use. (The **Approved** stamp is usually available directly in the menu that appears. Others are shown under *Dynamic, Sign Here, Standard Business*).
- Fill in any details and then click on the proof where you'd like the stamp to appear. (Where a proof is to be approved as it is, this would normally be on the first page).

or the business cycle, starting with the . on perfect competition, constant ret production. In this environment goods extra profits and the structure of market he model of the individual p determined by the model. The New-Keyotaki (1987), has introduced produc general equilibrium models with nomin

**APPROVED**

Drawing tools available on comment ribbon

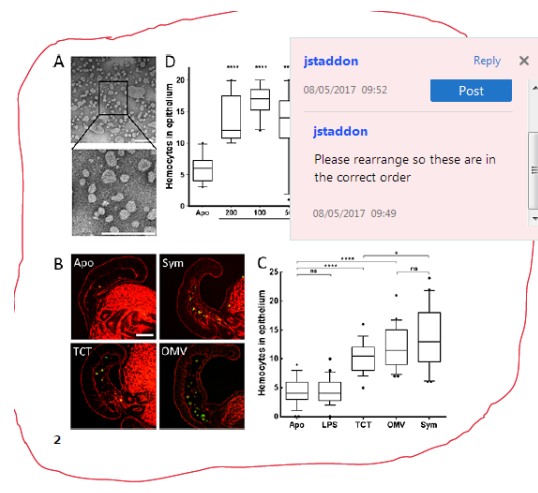


**How to use it:**

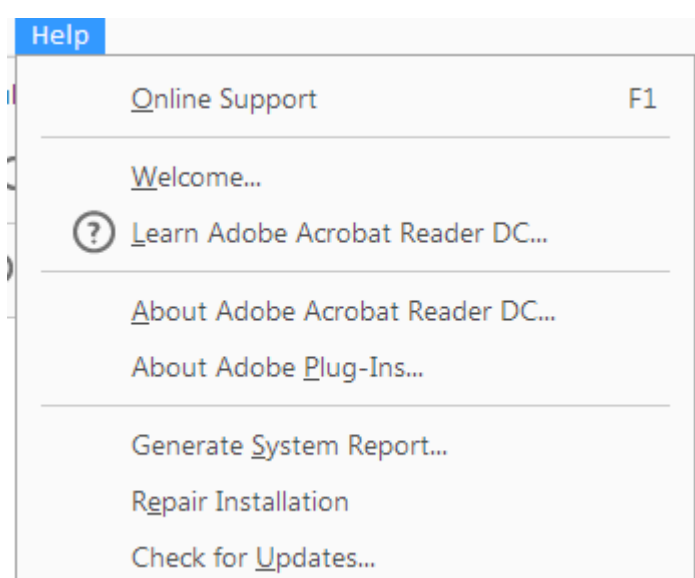
- Click on one of the shapes in the **Drawing Markups** section.
- Click on the proof at the relevant point and draw the selected shape with the cursor.
- To add a comment to the drawn shape, right-click on shape and select *Open Pop-up Note*.
- Type any text in the red box that appears.

**7. Drawing Markups Tools – for drawing shapes, lines, and freeform annotations on proofs and commenting on these marks.**

Allows shapes, lines, and freeform annotations to be drawn on proofs and for comments to be made on these marks.



For further information on how to annotate proofs, click on the **Help** menu to reveal a list of further options:



**PLEASE COMPLETE THE PUBLICATION FEE CONSENT FORM BELOW  
AND  
RETURN TO THE PRODUCTION EDITOR WITH YOUR PROOF CORRECTIONS**

Please return this completed form and direct any questions to the Wiley Journal Production Editor at TECTprod@wiley.com.

**To order OnlineOpen, you must complete the OnlineOpen order form at:**

[https://authorservices.wiley.com/bauthor/onlineopen\\_order.asp](https://authorservices.wiley.com/bauthor/onlineopen_order.asp)

Authors who select OnlineOpen will be charged the standard OnlineOpen fee for your journal, but excess publication fees will still apply, if applicable. **If your paper has generated excess publication fees, please complete and return the form below in addition to completing the OnlineOpen order form online (excess fees are billed separately).** If you would like to choose OnlineOpen and you have not already submitted your order online, please do so now.

**YOUR ARTICLE DETAILS**

**Journal:** *Tectonics*

**Article:** Wang, J., Mann, P., & Stewart, R. R. (2018). Late Holocene structural style and seismicity of highly transpressional faults in southern Haiti. *Tectonics*, 37, 1–19. <https://doi.org/10.1029/2017TC004920>

**OnlineOpen:** No      **Words:** 7,319      **Tables:** 0      **Figures:** 11      **Total Publishing Units:** 26

**Journal Base Fee:** \$0

**Excess Publishing Units:** 1@\$125    \$125

**Publication Fee Total:**        USD    \$125

**Please provide the information requested below.**

**Bill to:**

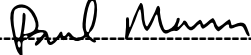
**Name:** \_\_\_\_\_

**Institution:** \_\_\_\_\_

**Address:** \_\_\_\_\_

**Phone:** \_\_\_\_\_ **Email:** \_\_\_\_\_

**Signature:** \_\_\_\_\_ **Date:** \_\_\_\_\_



An invoice will be mailed to the address you have provided once your edited article publishes online in its final format. Please include on this publication fee form any information that must be included on the invoice.

**Publication Fees and Length Guidelines:**

<http://publications.agu.org/author-resource-center/>

**Frequently Asked Billing Questions:**

[http://onlinelibrary.wiley.com/journal/10.1002/\(ISSN\)2169-8996/homepage/billing\\_faqs.pdf](http://onlinelibrary.wiley.com/journal/10.1002/(ISSN)2169-8996/homepage/billing_faqs.pdf)

**Purchase Order Instructions:**

Wiley must be listed as the contractor on purchase orders to prevent delay in processing invoices and payments.

## Author Query Form

---

**Journal: Tectonics**

**Article: tect20949**

Dear Author,

During the copyediting of your manuscript the following queries arose.

Please refer to the query reference call out numbers in the page proofs and respond to each by marking the necessary comments using the PDF annotation tools.

Please remember illegible or unclear comments and corrections may delay publication.

Many thanks for your assistance.

Query No.	Query	Remark
Q1	AUTHOR: Please complete the Publication Fee Consent Form included with your article and return to the Production Editor with your proofs.	
Q2	AUTHOR: Please confirm that given names (Blue) and surnames/family names (Vermilion) have been identified correctly.	
Q3	AUTHOR: Please verify that the linked ORCID identifiers are correct for each author.	
Q4	AUTHOR: Please check captions of Figures 1-10 if presented correctly.	
Q5	AUTHOR: Supporting information has been provided but has not been mentioned in the text. Please check.	We didn't provide supporting information. That probably was the Latex support file
Q6	AUTHOR: Please define InSAR if it is an acronym.	Interferometric Synthetic Aperture Radar
Q7	AUTHOR: Please provide publisher for Reference Bourgueil et al. (1988).	It is a technical report from Bureau of Mine and Energy (Bureau des Mines et de L'Energie) of Haiti.

## Tectonics

### RESEARCH ARTICLE

10.1029/2017TC004920

**Key Points:**

- First high-resolution sonar surveys of two actively deformed lakes in Haiti
- Extreme regional, tectonic transpression is partitioned by en echelon thrust faults and associated folds
- Three-dimensional deformation model integrates patterns of 2010 coseismic uplift, aftershock distribution, and mapped geologic structures

**Supporting Information:**[Supporting Information S1](#) **Correspondence to:**J. Wang,  
jwang61@uh.edu**Citation:**Wang, J., Mann, P., & Stewart, R. R. (2018). Late Holocene structural style and seismicity of highly transpressional faults in southern Haiti. *Tectonics*, 37. <https://doi.org/10.1029/2017TC004920>

Received 9 DEC 2017

Accepted 28 AUG 2018

Accepted article online 31 AUG 2018

## Late Holocene Structural Style and Seismicity of Highly Transpressional Faults in Southern Haiti

Jiannan Wang<sup>1</sup> ID, Paul Mann<sup>1</sup>, and Robert R. Stewart<sup>1</sup><sup>1</sup>Department of Earth and Atmospheric Sciences, University of Houston, Houston, TX, USA

**Abstract** The devastating 2010 Haiti earthquake ( $M_w$  7.0) was caused by rupture of the Léogâne, blind, thrust fault located 5 km north of the 1,200-km-long, left-lateral, Enriquillo-Plantain Garden fault zone (EPGFZ). Unexpectedly, the EPGFZ remained largely quiescent or slightly reactivated during the 2010 earthquake. Nevertheless, the EPGFZ still formed a major, crustal boundary between a coseismically uplifted lowland north of the EPGFZ and a subsided area in the highlands south of the fault. Here we use high-resolution sonar data from two Haitian Lakes that straddle the EPGFZ and its northern flank to demonstrate the presence of a 10- to 15-km-wide, 120-km-long, late Holocene fold-thrust belt which deforms clastic, lowland basins along the northern edge of the EPGFZ. In the eastern part of the study area, sonar results from Lake Azuey show that the linear trace of the EPGFZ cutting the Holocene lake bed is more deeply buried and less active than the adjacent, newly discovered, northwest striking, northeast dipping Jimani thrust fault that is part of the adjacent, transpressional belt of *en echelon* thrusts and folds. This structural relationship between a less active EPGFZ and more recently active, transpression-related Jimani thrust is remarkably similar to the 2010 epicentral area 70 km to the west between the less active EPGFZ and seismogenic Léogâne thrust during the 2010 Haiti earthquake. In this complex transpressional zone, we propose that coseismic deformation alternates at recurrence intervals of centuries between oblique, transpression-related structures (Léogâne, Jimani, and Trois Baies thrusts) and the main strike-slip, plate boundary fault zone (EPGFZ).

### 1. Tectonic Setting of the 2010 Haiti Earthquake

On 12 January 2010, a  $M_w$  7.0 earthquake struck the densely populated, greater Port-au-Prince region of south central Haiti and caused widespread destruction with over 230,000 fatalities and an estimated 10 billion dollars in damage (Bilham, 2010; Kocel et al., 2016; Paultre et al., 2013; Prentice et al., 2010; Figure 1). Multidisciplinary, geological, and geophysical studies within the 2010 epicentral area of south central Haiti include the following: (1) measurements and fault modeling of coseismic, coral reef uplift along a 50-km-long area of coastline in the epicentral region (Hayes et al., 2010); (2) coseismic, vertical ground motion from radar interferometry (Hashimoto et al., 2011); (3) high-resolution, surface fault trace mapping using Light Detection And Ranging and targeted field studies (Cowgill et al., 2012); (4) Global Positioning System (GPS) and 2010 aftershock-based studies and modeling of pre-, syn-, and post-2010 earthquake crustal motions (Calais et al., 2010; Douilly et al., 2015, 2013; Nettles & Hjörleifsdóttir, 2010; Symithe et al., 2013); (5) ground-based studies of Holocene scarps including coseismic ground fractures and late Quaternary scarps of the Enriquillo-Plantain Garden fault zone (EPGFZ) that remained unaffected by 2010 fault breaks (Koehler & Mann, 2011; Prentice et al., 2010; Rathje et al., 2014; Saint Fleur et al., 2015); (6) ground-based, near-surface, geophysical surveys of buried faults activated during the 2010 earthquake (Kocel et al., 2016); (7) near-coast surveys of submarine extensions of faults active in 2010 (Hornbach et al., 2010; Mercier de Lépinay et al., 2011); and (8) deepwater, marine surveys and coring to determine the recurrence interval of major earthquakes based on anomalous sedimentary deposits related to shaking and increased erosion (McHugh et al., 2011). The consensus from these previous, onshore and offshore, multidisciplinary studies is that the 2010 earthquake ruptured two previously unrecognized west to northwest striking thrust faults located 2 to 5 km north of the 1,200-km-long, left-lateral, EPGFZ that forms a major, plate boundary between the Caribbean plate to the south and the Gonâve microplate to the north (Benford et al., 2012; Calais et al., 2010; Corbeau et al., 2016; Mann et al., 1995) (Figures 1a and 1b). These two thrusts are separated by a distance of 6 km and include the following: (1) the subaerial, 8-km-long, blind, Léogâne thrust fault located 5 km north of the EPGFZ and trending at an angle

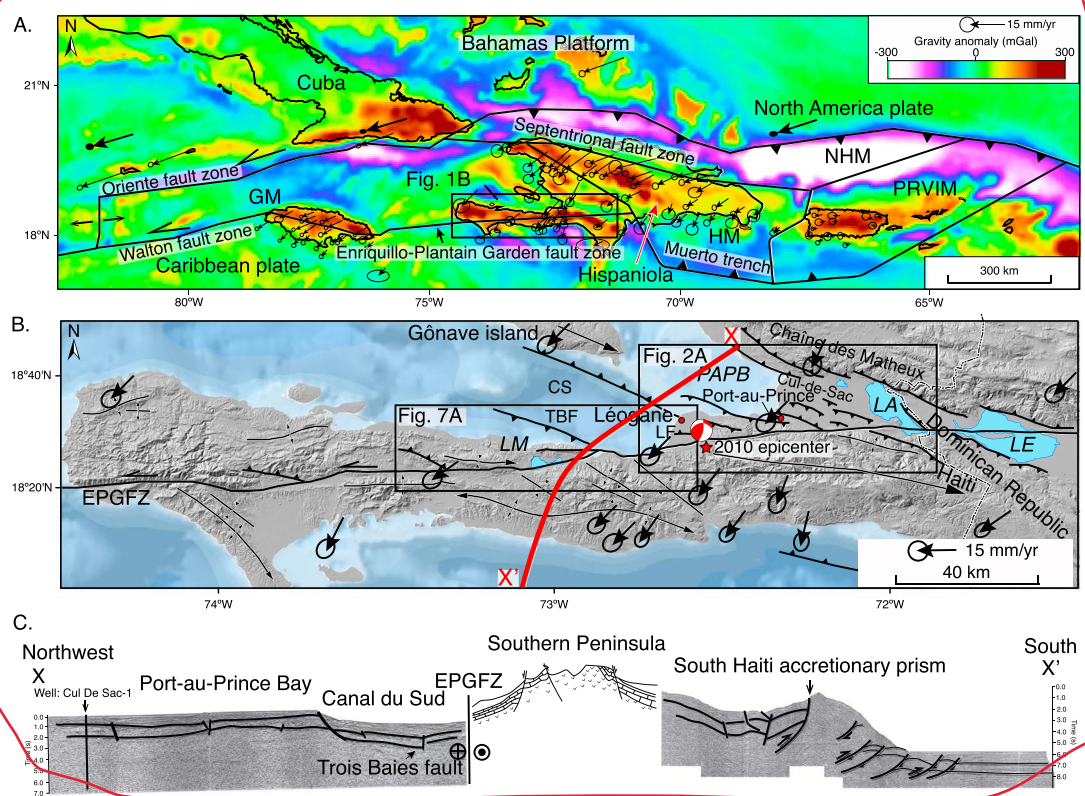


**Figure 1.** Tectonic setting of the northeastern Caribbean and Enriquillo-Plantain Garden fault zone (EPGFZ) in southern Haiti. (a) Free-air gravity anomaly map of the Greater Antilles (Cuba, Jamaica, Hispaniola, and Puerto Rico) in the northeastern Caribbean (<http://topex.ucsd.edu>) with gravity lows marking zones of subduction or thrusting along major faults (black lines) of the North America-Caribbean plate boundary. Arrows with error ellipses from Calais et al. (2010) are GPS vectors showing the direction and velocity of the large North American plate, the Bahamas platform, and intervening microplates relative to a fixed Caribbean plate. Microplates with variable relative motions occupy the 200-km-wide, transpressional, plate boundary zone and include the following: NHM = North Hispaniola microplate; HM = Hispaniola microplate; GM = Gonâve microplate; PRVIM = Puerto Rico-Virgin Islands microplate. Box shows more detailed map of the EPGFZ shown in (b). (b) Regional structure map of the southern peninsula of Haiti with the active, left-lateral Enriquillo-Plantain Garden fault zone (EPGFZ) from the Lake Enriquillo in the east to the western tip of the southern peninsula. The centroid moment tensor (CMT) mechanism is from Douilly et al. (2013). From east to west, key lakes and marine embayments aligned parallel and overlying the EPGFZ include the following: LE = Lake Enriquillo, Dominican Republic; LA = Lake Azuey, Haiti; PAPB = Port-au-Prince Bay; CS = Canal du Sud; TBF = Trois Baies fault; LM = Lake Miragoâne; LF = Léogâne fault. Boxes show more detailed maps of the structure of the EPGFZ and its secondary faults shown in Figures 2a and 7a. (c) Composite, multichannel seismic reflection line (acquired by Canadian Superior Energy Inc.) located as the red line X-X' in (b) that shows an unfolded area of high-angle faults in the Canal du Sud tied to the offshore Cul De Sac-1 well, the Trois Baies fault, the EPGFZ, the anticlinal structure of the southern peninsula, and a large, south verging accretionary prism along the south coast of the southern peninsula. The depth scale for this section is in two-way, travel time.

of  $8^\circ$  to the EPGFZ (Calais et al., 2010; Douilly et al., 2013, 2015, 2017) and (2) the submarine, 20-km-long Trois Baies thrust fault located 2 km north of the EPGFZ and trending at an angle of  $20^\circ$  to the EPGFZ (Mercier de Lépinay et al., 2011; Symithe et al., 2013; Figures 1b and 1c).

Despite the proximity of the Léogâne and Trois Baies thrust to the neighboring EPGFZ, the EPGFZ remained largely quiescent and outside the zone of maximum, coseismic uplift and ground shaking and aftershocks produced by the 2010 earthquake (Nettles & Hjörleifsdóttir, 2010). The centroid moment tensor mechanism of the main 2010 shock shows a primarily strike-slip motion, with a small component of reverse motion, on a steeply north dipping nodal plane (Douilly et al., 2013; Nettles & Hjörleifsdóttir, 2010). Finite element modeling (Douilly et al., 2015) suggests that Léogâne fault that is buried beneath at least 1 km of overlying undeformed clastic sediment in the area north of the EPGFZ absorbed northeast-southwest shortening related to extreme transpression along obliquely striking, high-angle ( $21\text{--}70^\circ$  dipping) reverse fault planes. For this reason, there was insufficient stress to trigger slip during the 2010 earthquake on the more east-west striking

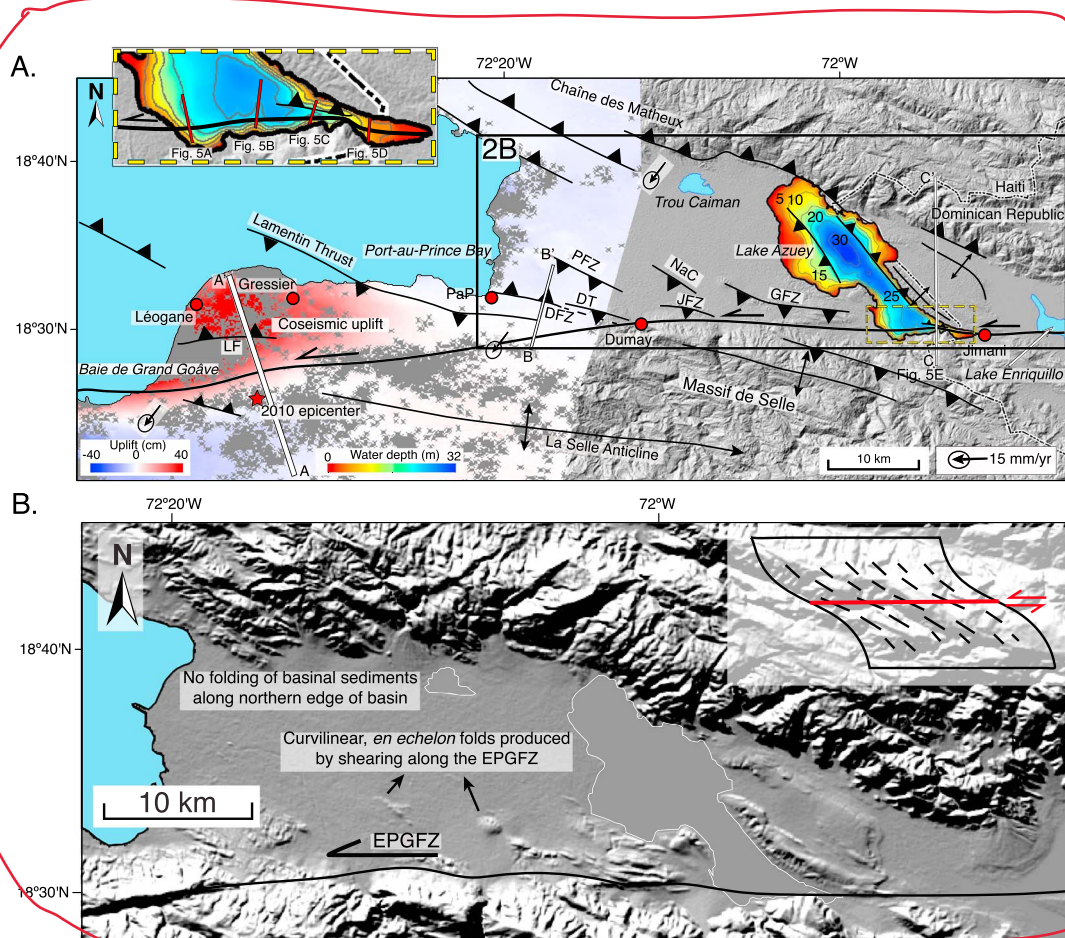


**Figure 2.** Structure of the EPGFZ in eastern Haiti. (a) Faults and folds along a 15-km-wide corridor parallel to the EPGFZ superimposed on a modified DEM and InSAR surface deformation map (courtesy of Eric Fielding at JPL; Hayes et al., 2010). Chirp bathymetry of the Lake Azuey is also shown. GPS vectors are from Calais et al. (2010). PFZ = Port-au-Prince fault zone; DFZ = Dumay fault zone; DT = Dumay thrust; NaC = Nan Cadastre thrust; JFZ = Jacquet fault zone; GFZ = Ganthier fault zone; LF = Léogâne fault; EPGFZ = Enriquillo-Plantain Garden fault zone; DEM = digital elevation model. Line A–A': Cross section along the blind Léogâne thrust fault (shown in Figure 3); Line B–B': Cross section of north Port-au-Prince urban area (shown in Figure 3). (b) Shaded DEM [northern deformed belt in the Cul-de-Sac basin with northeastern illumination from Figure 2a showing **en echel**] curvilinear folds striking west-northwest obliquely with respect to the EPGFZ and plunging beneath undeformed sediments occupying the center of the Cul-de-Sac Valley. The inset schematic diagram of shearing along a strike-slip fault is from Odonne and Vialon (1983).

EPGFZ located 5 km to the south (Figure 1b). Previous GPS surveys (Calais et al., 2016) along this area of the EPGFZ have shown that plate motion is almost at right angles to these obliquely striking thrusts and consistent with their preferred orientation for reactivation within the area of northeast-to-southwest shortening (Figures 1a and 1b).

Aftershock studies following the 2010 earthquake by Douilly et al. (2015, 2016) showed that the EPGFZ moved locally at depth and acted as a 6-km-long, east-west and subvertical, connecting fault segment that transmitted seismogenic motion between the obliquely trending, north dipping, Léogâne fault in the east and the more obliquely trending, southwest dipping Trois Baies fault in the west (Figure 1b). However, postearthquake geologic reconnaissance revealed no fault-related, surface ground breaks along the proposed onland areas of EPGFZ in the epicentral region of the earthquake (Koehler & Mann, 2011; Prentice et al., 2010; Rathje et al., 2014). A more recent study by Saint Fleur et al. (2015) proposed previously unrecognized, 2010 coseismic groundbreaks along the obliquely trending Lamentin thrust 11 km east of the epicentral area near the city of Port-au-Prince (Figure 2a).

**En echel** exists spacing at distances of 1–8 km along the main strike-slip fault obliquely intersects the main strike-slip fault at angles of 30–45°. These structures strike northwestward away from the EPGFZ for

distances of 4–29 km into the more thickly sedimented basinal areas north of the EPGFZ (Figure 2a). As a result of this distinctive and regular intersecting fault geometry between these oblique thrusts and the linear EPGFZ, earthquake rupture initiating on an oblique thrust, as seen for the Léogâne fault in 2010, is likely confined to that northern ~~vicinity~~ and may not connect with other oblique thrusts or even the EPGFZ itself (Douilly et al., 2015, ).

Coseismic deformation along a large transpressional strike-slip fault, such as the EPGFZ (Calais et al., 2002) in Hispaniola or the San Andreas fault zone in California (Segall & Lisowski, 1990), is either accommodated by (1) slip and major earthquakes on the main, strike-slip plate boundary fault; (2) the oblique, en echelon thrusts adjacent to the main fault; (3) or both sets of faults (cf. compilation of types of destructive earthquakes in transpressional settings by Hayes et al., 2010). Motions on distributed, en echelon thrusts do not necessarily spare or reduce coseismic rupture on the main strike-slip fault because the en echelon and main strike-slip fault remain separate fault planes, and the main strike-slip fault would continue to accumulate strain. In an extreme transpression case as observed in Haiti, plate motions become increasingly convergent across the main, strike-slip fault zone (Figures 1a and 1b). In such a setting, the en echelon, oblique thrusts might assume more and more plate edge strain to the point that the plate boundary behaves more like a broad, thrust boundary and less like a narrow, strike-slip boundary (Mount & Suppe, 1987).

These oblique and en echelon thrust faults in transpressional settings, which include large restraining bends such as Hispaniola, potentially nucleate *uncharacteristic earthquakes* of varying recurrence intervals and sizes that are distinct from the recurrence intervals and sizes of the adjacent but independent strike-slip faults (Fielding et al., 2013). Restraining bend areas like Hispaniola can lead to the generation and increased activities on more favorably and obliquely oriented folds and thrusts whose coseismic rupture might alternate with much longer ruptures along the adjacent strike-slip fault. The number of these en echelon thrust faults can be large at observed spacings of 5–10 km dispersed along the trend of strike-slip faults that may be hundreds of kilometers in total length. For this reason, the identification and earthquake potential of oblique en echelon thrusts, especially when buried or “blind”, can be challenging to assess in transpressional zones (Frankel et al., 2011).

## 2. Objectives and Methods

### 2.1. Study Area

The elongate belt of transpressional deformation associated with en echelon thrusts occupies a topographically low, densely populated Cul-de-Sac basin underlain by poorly consolidated, clastic sedimentary rocks ranging in age from Miocene to recent (Mann et al., 1995; Massoni, 1955; Saint Fleur et al., 2015; Terrier et al., 2014). In easternmost Haiti, this belt is overlain by the shallow (33 m deep), 138 km<sup>2</sup>, brackish Lake Azuey near the border separating Haiti from the Dominican Republic (Piasecki et al., 2016; Wright et al., 2015). Lake Enriquillo to the east is twice as large (346 km<sup>2</sup>) as Azuey, shallow (52 m deep), hypersaline, about 40 m below sea level and located entirely in the Dominican Republic. Lake Enriquillo is separated from Lake Azuey by the eastward continuation of the same transpressional belt parallel and north of the EPGFZ in the Cul-de-Sac valley (Mann et al., 1995; Figure 1b).

In the western part of our study area, the more transtensional segment of the EPGFZ is overlain by the 42.8-m-deep, 14 km<sup>2</sup>, freshwater Lake Miragoâne (Figure 1b). All three of these shallow, inland, lakes experience variations up to 13 m in their surface elevations due to annual to decadal changes in climate and rainfall amounts including extreme rainfall events associated with hurricanes (Moknatian et al., 2017; Piasecki et al., 2016; Rico, 2017; Wright et al., 2015).

### 2.2. Objectives

The main goal of this paper is to better integrate the geologic structure of the 120-km-long study area, which parallels the trace of the EPGFZ and includes the 2010 epicentral area. Data types that we have integrated for this study include the following: surficial geologic mapping, geophysics, GPS, radar interferometry, aftershocks, and modeling studies. Most of these studies were completed in the aftermath of the 2010 earthquake. Our study integrates these data sets in order to structurally characterize the 10- to 15-km-wide, belt of late Holocene, transpressional deformation that forms a laterally extensive, deformed belt along the inland, Cul-de-Sac intermontane basin in the east and the low-relief coastal plain along Port-au-Prince ~~bay~~ and the Canal du Sud to the west (Figure 1b). In particular, we focus on identifying a family of en echelon thrusts, whose curvilinear strikes area are very similar to the Léogâne thrust now known to be responsible for most

of the energy release and coseismic uplift during the 2010 Haiti earthquake (Calais et al., 2010; Douilly et al., 2015; Figures 1b and 2a).

### 2.3. Survey Design

In order to understand the geologic and structural styles of transpression within this belt, including the age relations between deformation in the north flanking belt and the EPGFZ itself, we collected a total of 94 km of high-resolution (2–10 kHz) sonar profiles in 2014 from the 138-km<sup>2</sup> brackish Lake Azuey and 37 km of profiles from the 14-km<sup>2</sup> freshwater Lake Miragoâne (Figure 1b). The EPGFZ strikes through both of the lakes, so 80% of our lines on Lake Azuey and 90% of our survey lines on Lake Miragoâne were dedicated to the across fault-strike, north-south profiles.

The average speed of the small, outboard, motorboat towing the sonar was 3 knots, with a sonar pulse rate of 4 s<sup>-1</sup>. Our 2- to 10-kHz sonar frequency range yielded sub-bottom layer resolution of about 10 cm (Wang & Stewart, 2015). These surveys were the first sonar surveys in Haitian Lakes. Both lakes straddle the projected active trace of Haiti's EPGFZ and its adjacent, transpressional fold-thrust belt and therefore provide new constraints on the location, structural style, and timing of deformation within both structural provinces. We integrate these lake data with previous geologic mapping, geophysical observations related to the 2010 earthquake, and regional information on plate motions in this region.

## 3. Tectonic Setting of Transpressional Deformation in South Central Haiti Including Unresolved Tectonic and Structural Questions

### 3.1. Previous Strike-slip Deformational Model Versus Haiti Thrust Belt Deformational Model

There are two, previously proposed, regional structural models to explain the present-day structure of the broad, 250-km-wide zone of transpression spanning the entire width of the island of Hispaniola.

#### 3.1.1. Strike-Slip, Regional Structural Model

The first is the strike-slip dominated model driven by oblique motion and transpression between the thick and buoyant Bahamas platform on the North America plate, the Caribbean plate, and the Gonâve microplate (Calais et al., 2002, 2016; Dolan et al., 1998; Mann et al., 2002, 2010; Figures 1a and 1b). GPS surveys within this 250-km-wide transpressional zone (Calais et al., 2010, 2002; Douilly et al., 2015; Hayes et al., 2010; Symithe et al., 2013) reveal strain partitioning along the EPGFZ and the subparallel Septentrional strike-slip fault zone 200 km to the north (which is the plate boundary separating the North Hispaniola microplate and Gonâve microplate; Figure 1a). As a result of this oblique collision and restraining bend area, the 3-km-high mountains of central Hispaniola have grown since the late Miocene to an elevation of 3 km to the highest range in the northern Caribbean.

The left-lateral strike-slip rupture of the EPGFZ in the eighteenth century inferred from the map pattern of historical earthquakes (Bakun et al., 2012) combined with average late Holocene, left-lateral offset amounts of 1.3–3.3 m as expressed along offset streams of the EPGFZ (Prentice et al., 2010) and by late Holocene, left-lateral channel offsets of 7–8 m along stream channels offset by the Septentrional fault zone (Prentice et al., 2003, 1993).

The study by Saint Fleur et al. (2015) indicates that the folding and thrusting of 10- to 15-km-wide belt of Miocene to Quaternary rocks were generated by transpression along the EPGFZ. In addition, Mann et al. (2002), Grindlay et al. (2005), and...eller et al. (2011) suggest a strong, southwestward, back thrusting of the southern Hispaniola in Haiti and Dominican Republic to the southwest onto the Caribbean plate (Figures 1b and 1c). Southwestward back thrusting of Hispaniola is manifested by the large accretionary wedge along the Muerto trench south of the Dominican Republic (Bien-Aimé Momplaisir, 1986; Bruña et al., 2009; Figures 1a and 1b) and along the southern margin of Haiti (South Haiti accretionary prism; Bien-Aimé Momplaisir, 1986; Figure 1c). A localized, negative gravity anomaly marks the trend of plate flexure of the underthrusting Caribbean plate beneath the overriding area of southern Hispaniola (Bruña et al., 2009; Mann et al., 2002; Figure 1a).

#### 3.1.2. Criticisms of the Strike-Slip, Regional Structural Model

Two criticisms have been proposed for the strike-slip model. First, Corbeau et al. (2016) noted that the predictions of the GPS-based block models overestimate the observed amounts of transpression-related shortening seen on seismic reflection profiles in the offshore area of the Gulf of Gonâve north of the southern peninsula of Haiti or in the area of the Jamaica Passage east of Haiti. Second, Symithe and Calais (2016) have proposed

that there is no geologic evidence for a continuation of the EPGFZ east of latitude 72.27°W in the eastern Cul-de-Sac Valley, Lake Azuey, and Lake Enriquillo in the Dominican Republic (Figure 1b). Instead, Symithe and Calais (2016) propose that the high rates of north-south shortening predicted from GPS block models are accommodated entirely by low-angle thrust structures in the eastern Cul-de-Sac and Enriquillo Valleys that were modeled using GPS data as part of their study.

### 3.1.3. Trans-Haitian Fold-and-thrust Belt Regional Structural Model

The Trans-Haitian fold-and-thrust belt model originated with a study by Pubellier et al. (2000), who proposed a low-angle southwestward verging fold-and-thrust belt along the southwestern edge of the central Hispaniola block. The thrust front of this feature was thought to be actively propagating from the main Trans-Haitian fold-and-thrust belt that is located in the Chaîne des Matheux (Figures 1b and 2a), southwestward into the area of the Léogâne plain and the Cul-de-Sac basin (Figures 2a and 2b). Pubellier et al. (2000) proposed that the EPGFZ originally formed as a left-lateral strike-slip fault but became inactive in the late Miocene when deformation in southern Hispaniola became inactive. Increasing amounts of shortening caused the Trans-Haitian fold-and-thrust belt to propagate into the southern area of the Cul-de-Sac basin and Léogâne plain, where it emerged or ~~day~~ to form the en echelon, convergent structures (compiled on the map in Figure 2). Pubellier et al. (2000) also proposed that the EPGFZ was reactivated as a normal fault in the Quaternary as a result of crustal loading of the southern, foreland area by the overthrusting Trans-Haitian fold-and-thrust belt.

Following the 2010 earthquake and the recognition of the north dipping blind Léogâne thrust fault, Calais et al. (2010) proposed that the Léogâne fault marks the leading edge of the Trans-Haitian fold-and-thrust belt rather than ~~being an~~ en echelon thrust genetically linked to the EPGFZ. In the interpretation proposed by Calais et al. (2010), the northward dip of the Léogâne thrust made it difficult to link its origin with the EPGFZ, whose dip had been established in this area as a vertical to high angle (>60°), south dipping fault plane with evidence of late Holocene, left-lateral offsets of drainages (Prentice et al., 2010). Moreover, Symithe and Calais (2016) noted that Trans-Haitian fold-and-thrust belt regional model of Pubellier et al. (2000) was more consistent with GPS data showing larger magnitude, north-south shortening in central Hispaniola than with the existence of an eastward extension of the left-lateral EPGFZ into the eastern part of Haiti and the Dominican Republic (Figures 1b and 2a).

### 3.1.4. Criticisms of the Trans-Haitian Fold-and-Thrust Belt, Regional Structural Model

First, Mercier de Lépinay et al. (2011) pointed out two problems with linking the origin of the Léogâne thrust to the southwestward propagating edge of the Trans-Haitian fold-and-thrust belt: (1) the dip of the fault generating the main thrust, as imaged by Mercier de Lépinay et al. (2011), was more steeply dipping (64°) than expected for a blind thrust at the leading edge of a fold-thrust belt and (2) the orientation of the N84°E fault plane of the main shock is significantly oblique to the N120°E oriented leading edge of the Trans-Haitian fold-and-thrust belt as proposed by Pubellier et al. (2000). In this paper, we discuss other inconsistencies with the previous interpretation that deformation north of the EPGFZ is the result of southwestward propagation of the Trans-Haitian fold-and-thrust belt.

## 4. New Observations of the Late Holocene Structural Style Along EPGFZ in Southern Haiti

### 4.1. Significance of En Echelon Thrusting and Folding North and South of the EPGFZ

The presence of a strike-slip fault at any scale is indicated by the presence of en echelon arrays of thrust faults, normal faults, folds, fractures, dikes, and other linear features in narrow, elongate zones (Sylvester, 1988). In Figure 2a, we have compiled geologic information on en echelon folds and faults in a 10- to 15-km-wide zone of deformation along both the northern and southern flanks of the EPGFZ. Folds form as fault propagation folds along oblique, thrust faults, vary from 1 to 8 km in lateral spacing, and deform Miocene and younger fine to coarse-grained, basinal, and coastal plain rocks in the belt that is 10–15 km wide and extends parallel to the EPGFZ for 120 km (Figures 1b and 2a). Folds in Neogene clastic lithologies of the Cul-de-Sac basin contrast with more continuous and longer wavelength, en echelon fold axes present in more massively bedded Cretaceous to Eocene rigid, basaltic, and carbonate lithologies exposed in the 2-km-high range south of the EPGFZ, the Massif de Selle (Figure 2a). The curvilinear trend of fold axes is similar both to the north and south of the EPGFZ and indicates a genetic relation between left-lateral shearing along that fault and the formation of those en echelon features (Figure 2b).

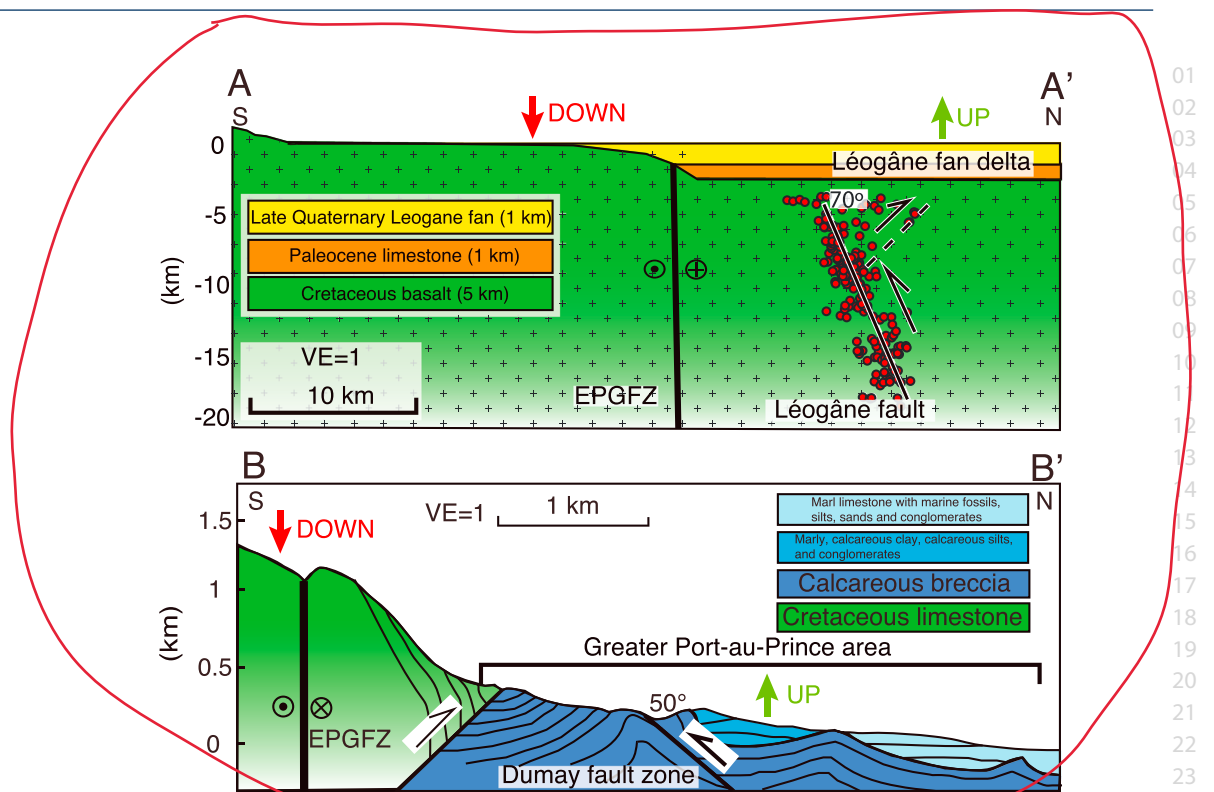


**Figure 3.** Style of late Neogene, transpressional deformation in the Cul-de-Sac basin along two transects shown in Figure 2. (A–A') Aftershocks of the 2010 earthquake (Douilly et al., 2015, 2013) along the blind Léogâne thrust fault reveal conjugate reverse faults with the dominant slip occurring on the north dipping fault. The red triangle indicates the location of Léogâne city. Coseismic uplift during the 2010 earthquake elevated the northern basinal area and depressed the mountains south of the EPGFZ. (B–B') Cross section based on surface mapping (Cox et al., 2011; Massoni, 1955; McHugh et al., 2011; Saint Fleur et al., 2015) showing both north and south dipping reverse faults deforming Plio-Pleistocene sedimentary rocks. EPGFZ = Enriquillo-Plantain Garden fault zone.

The en echelon distribution of complex Holocene folding and thrusting in the 10- to 15-km-wide zone of deformation north of the EPGFZ is also reflected in the complex pattern of 2010 coseismic and vertical deformation recorded by the interferogram from the 2010 epicentral area on the Léogâne plain west of the Cul-de-Sac basin (Bilham & Fielding, 2013; Hashimoto et al., 2011; Hayes et al., 2010; Figure 2a). Douilly et al., (2013, 2015) and Kocel et al. (2016) use aftershocks and shallow geophysics to show that the 2010 Léogâne thrust fault and subparallel faults are overlain by at least 1 km of undeformed and subhorizontal strata (cross-section A–A' in Figure 3).

#### 4.2. Significance of Curvilinear Fold and Thrust Patterns in the Transpressional Belt North of the EPGFZ

The shaded relief digital elevation model shown in Figure 2b reveals the curvilinear, en echelon fold morphologies that are defined by low, bedrock hills of Neogene sedimentary rocks exposed on the flat-lying Cul-de-Sac basin. These curvilinear fold axes can be related directly to a broad zone of left-lateral, simple shear produced along the subvertical and left-lateral EPGFZ based on several, basic observations seen in Figure 2b. The most prominent folds present along the southern edge of the Cul-de-Sac basin are within 15 km of the EPGFZ. In contrast, the central and northern edges of the Cul-de-Sac basin exhibit no prominent folding, even directly adjacent to the base of Eocene-Miocene carbonate rocks forming the range (Pubellier et al., 2000; Figure 2a). The map view shapes of fold axes along the southern margin of the Cul-de-Sac basin are asymptotic or gently curve into east-west parallelism with the main trace of the EPGFZ along the southern edge of the Cul-de-Sac basin, as observed in claybox experiments of shearing (see the inset of Figure 2b; modified from ; Odonne & Vialon, 1983). Deeper, structural depressions form in the zone of convergent intersection between the east-west striking EPGFZ and the northwest striking, secondary thrusts as seen in the southern part of Lake Azuey, where the lake bends from an east-west trend adjacent to the EPGFZ to a more northwest trend in the central and northern parts of the basin (Figures 2a and 2b).

#### 4.3. Geologic Structure of the Area of En Echelon Thrusts in the Epicentral Area on the Léogâne

##### Fan-Delta

##### 4.3.1. Geologic Structure of the Léogâne Fan Area

A cross-sectional profile of the 2010 epicentral area related to the activation of two conjugate thrust faults is modified from aftershock data from Douilly et al. (2013, 2015) and is shown in Figure 3 (Line A–A'). Both faults are buried by about 1 km of late Quaternary sand and gravel of the Léogâne fan delta (Kocel et al., 2016) and an additional 1 km of Paleocene limestone. Aftershocks indicate that the main thrust event ruptured a depth range from 4 to 17 km beneath the ground surface (Douilly et al., 2015, 2013). The orientation of the Léogâne thrust based on gravity and uplift of coastal features is east-west and parallel to recent near-surface breaks of the EPGFZ mapped in the shallow, coastal zone adjacent to the Léogâne plain (Hornbach et al., 2010). Due to its proximity to the EPGFZ, an east-west strike of the Léogâne thrust is predicted as this is the area where en echelon folds and faults curve into an asymptotic orientation relative to the main EPGFZ, as shown in Figure 2b.

A radar interferogram compiled on the structure map of Figure 2a revealed that the 2010 earthquake elevated the smaller folds of the Léogâne fan delta north of the EPGFZ yet produced coseismic subsidence in the 1.4-km-high, less complexly deformed, mountain range south of the EPGFZ (Hashimoto et al., 2011; Figure 2a). This paradox can be simply explained by the northward dip of the seismogenic Léogâne fault that elevated the basinal area to the north (hanging wall of the Léogâne fault) and depressed the mountainous area to the south (footwall block of the Léogâne fault (line A–A' in Figure 3).

##### 4.3.2. Geologic Structure of the Port-au-Prince Urban Area Compared to the Léogâne Epicentral Area

A similar pattern of deformation is observed in Port-au-Prince urban area where the central and northern edge of the Cul de Sac basin is only gently folded and faulted (Cox et al., 2011; Massoni, 1955; McHugh et al., 2011; Saint Fleur et al., 2015, Line B–B' in Figure 3). The cross section taken from workers, who were mapping 60 years ago when Port-au-Prince was smaller and the geology was less obscured by urbanization, shows two large thrusts, a range-bounding thrust along the southern edge of the city and a northeast dipping thrust, the Dumay thrust, that elevates a broad outcrop zone of north-dipping, Neogene sedimentary rocks on which the northern area of Port-au-Prince is built (Rathje et al., 2014). The 50° northeast dip of the Dumay thrust is similar to the 70° northeast dip of the Léogâne thrust to the west known from aftershocks (Douilly et al., 2015, 2013), though the dip of the Dumay thrust reverses to a southwest dip as it approaches the EPGFZ (Figures 2a and 2b).

On the cross section B–B' in Figure 3, we have indicated areas that are elevated as a result of the northward dip of the Dumay thrust and the depression of the area to the south of the EPGFZ in the highlands south of the EPGFZ. If a future earthquake occurred along the north-dipping, en echelon thrust faults in the Port-au-Prince area (Line B–B' in Figure 2) or Lake Azuey area (Line C–C' in Figure 2), a similar uplift phenomenon is likely to occur where the lowlands north of the EPGFZ are uplifted and the adjacent mountains south of the EPGFZ subside.

##### 4.3.3. Geologic Structure of the Lake Azuey Area

In the Lake Azuey area, we mapped a linear, 250- to 500-m-wide, and east-west striking fault trace in deformed Holocene sediments along the projected trend of the landward traces of the EPGFZ both east and west of Lake Azuey (Figures 4 and 5a–5d). The fault is marked by a 250- to 500-m-wide, graben-like feature that disrupts the uppermost late Holocene, lake stratigraphy. Integrated with previous land mapping of the EPGFZ (Bourguiel et al., 1988; Cowgill et al., 2012; Mann et al., 1995; Prentice et al., 2010), we interpret this linear east-west striking feature in Lake Azuey as a 250- to 500-m-wide and continuous trace of the EPGFZ which we can follow westward to the EPGFZ locality at Dumay, about halfway between Lake Azuey and Port-au-Prince, which was previously described and dated as a 6-m-long, left-lateral offset of a late Holocene stream channel (Cowgill et al., 2012; located at red circle, which is labeled as Dumay in Figure 2a). A similar, 500-m-wide, graben-like structure was described by Hornbach et al. (2010) along the trace of EPGFZ where it enters the Baie de Grand Goâve 75 km west of Lake Azuey (Figure 2a).

The structural cross sections in this area were compiled from previous studies (Douilly et al., 2015; Mann et al., 1995; Massoni, 1955) and indicate that the high-angle EPGFZ coexists with the adjacent thrusts that over-thrust from the south and north (Line B–B' in Figure 3). We project this trace of the EPGFZ along a prominent fault valley at the town of Jimani that separates Lakes Azuey and Enriquillo (Figures 2a and 4). Sonar profiles (Figures 5a–5d) show that the most recent rupture of the EPGFZ is covered by about 0.7 m of Holocene

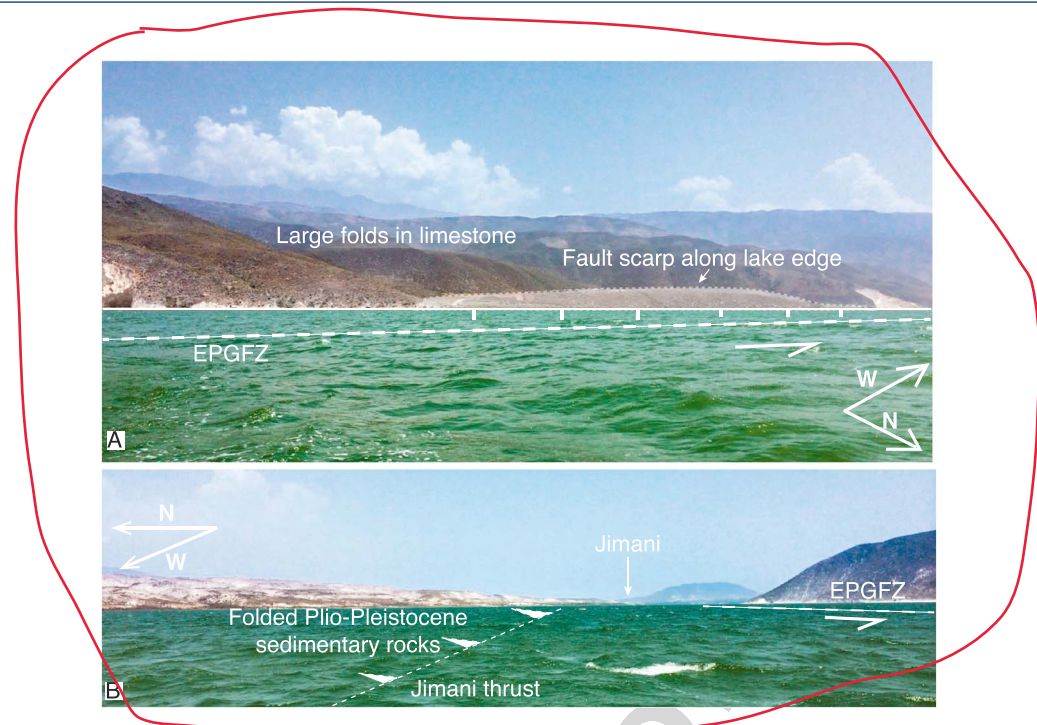


**Figure 4.** Geologic setting of Lake Azuey, Haiti. (a) To the south, the green-colored, brackish waters of Lake Azuey are bound by the EPGFZ which forms a sharp boundary with 2-km-high folded limestone of Paleogene age that forms the smooth surfaces on the skyline. A fault strand of the EPGFZ marks the south edge of Lake Azuey, while other parallel strands of the EPGFZ underlie the southern part of the lake as schematically shown. (b) To the north of the lake folded, Plio-Pleistocene strata form the uplifted, 0- to 30-m-high isthmus that separates Lake Azuey (15-m ASL) from Lake Enriquillo (46-m BSL) located 1 km to the east. Approximate locations of the EPGFZ and the Jimani thrust fault are shown. EPGFZ = Enriquillo-Plantain Garden fault zone.

sediment, suggesting that there has been late Holocene activity of the EPGFZ along the southern edge of the lake.

From sonar data, we observed late Holocene lake sediments onlapping onto local highs of Eocene limestone of the bounding range along the northern edge of the EPGFZ, indicating that this margin is not controlled by late Holocene faulting (Figures 5c and 5e). The sonar from southern Lake Azuey suggests that the most prominent folds present adjacent to the EPGFZ become less prominent in the central and northern parts of the lake (Figure 2b). These southern folds and thrusts imaged in Lake Azuey define the transpressive belt along the EPGFZ observed in onshore areas to the west. On the cross section in Figure 5e, we have schematically indicated areas that are elevated as a result of the northward dip of the Jimani thrust and the depression of the area to the south of the EPGFZ.

The structural cross section (Figure 5e) of the Lake Azuey area and the previous works (Bourqueil et al., 1988; Cox et al., 2011; Douilly et al., 2015; Massoni, 1955; Lines A–A' and B–B' in Figure 3) along this 120-km-long zone of deformation adjacent to the EPGFZ shows that the oblique thrust faults share a similar orientation with other northeast dipping thrusts along the northern edge of the EPGFZ. All three of these oblique thrust faults (the Léogâne thrust in Line A–A', the Dumay thrust in Line B–B', and the Jimani thrust in Figure 5e) shown on the cross sections deform rocks as young as Pliocene and Quaternary (Saint Fleur et al., 2015).

On a more regional scale, these observations from Lake Azuey are consistent with the multichannel seismic reflection profile (named as Canadian Superior 2-D and shown in Figure 1c) that shows a lack of intensive deformation in the part of Port-au-Prince Bay that is the offshore, largely unfaulted and folded seaward extension of the Cul-de-Sac basin (McHugh et al., 2011). Pubellier et al. (2000) propose that the Trans-Haitian fold-and-thrust belt exposed in the Chaine des Matheux range extends beneath the entire Cul-de-Sac and Port-au-Prince basins (Figures 2a and 2b). In summary, our observations at this scale do not support the previous model by Pubellier et al. (2000) and Calais et al. (2010) that folds and faults of the northern range are propagating southwestward beneath the zone of en echelon faults and folds (Figures 2a and 2b).

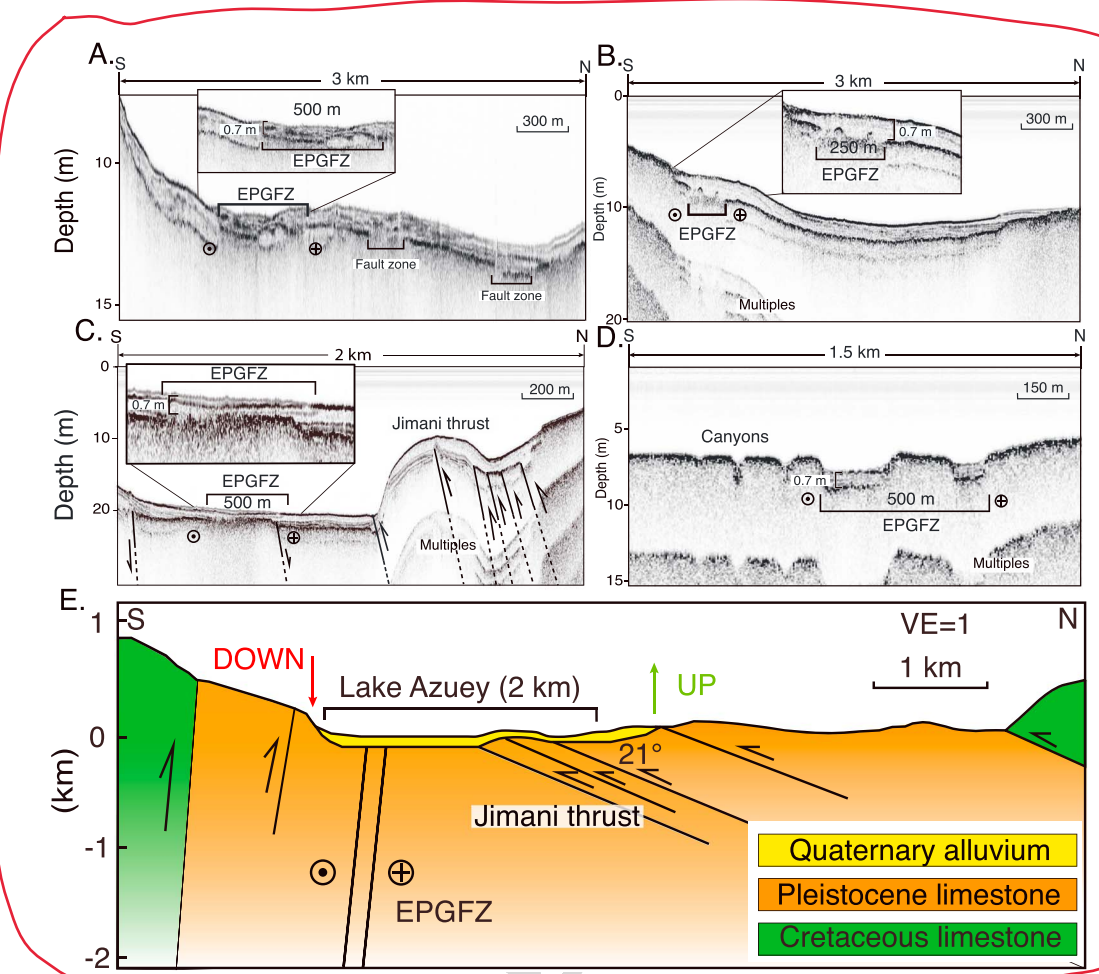


**Figure 5.** Chirp sonar profiles showing the trace of the EPGFZ in the southern part of Lake Azuey and its relationship with a newly described thrust we have named the Jimani thrust. (a–d) Cross sections indicated in Figure 2a. The EPGFZ beneath Lake Azuey forms a 250- to 500-m-wide zone that can be traced as a lineament to the east and west of Lake Azuey (Figure 2). The green and red horizons represent two distinguish stratigraphic layers. The two strands of the EPGFZ are buried by 0.7 m of Holocene sediment and are extrapolated to be 270 years old since their last rupture when an average sedimentation rate of 2.6 mm/year based on cores from Lake Enriquillo is assumed. Folds associated with the Jimani thrust are interpreted as fault propagation folds above northeast dipping thrust faults. (e) Cross section based on both sonar survey and the surface mapping (Mann et al., 1991) showing north and south dipping, reverse faults deforming Plio-Pleistocene sedimentary rocks. EPGFZ = Enriquillo-Plantain Garden fault zone.

#### 4.4. Subsurface Stratigraphy of Lake Azuey and Lake Enriquillo and Paleoseismic Estimates of the Relative Timing of Recent Earthquakes on the EPGFZ and Secondary, En Echelon Thrust Faults

Our objective is to determine the relative age of the EPGFZ and its adjacent zone of fold-and-thrust deformation using the sonar profiles from Lakes Azuey and Enriquillo (Figure 6a). Previous coring, both in Lake Enriquillo (Rios et al., 2013; which was tied to the onshore stratigraphic studies; Rios et al., 2013; Taylor et al., 1985) and in Lake Miragoâne (Higuera-Gundy et al., 1999), has established the late Holocene history in the upper 5 and 7-m sediments, respectively.

In Lake Enriquillo, a sonar survey similar to ours was conducted in 2013 (Rios et al., 2013). Mapping in both lakes revealed the presence of the east-west, subparallel strands of the EPGFZ that are collinear with onland scarps both east and west of Lake Azuey (Figures 2 and 4) and east and west of Lake Enriquillo (Mann et al., 1995; Rios et al., 2013; Figure 6a). These east-west fault strands abruptly truncate the trends of folds in the ranges south of the lake (Figure 4). The sonar events, which are interpreted as stratigraphic features, from Lake Azuey and Lake Enriquillo (Lines B1 and L19 correlate convincingly; Figure 6b). Schwartz (1980) suggested that both lakes were the results of the closure of former marine straits. Due to the small distance separating the two lakes (about 4 km), the two lakes merged during heavy rainfall years (Greer & Swart, 2006; Medley et al., 2007; Romero Luna & Poteau, 2011). Given the similarity of the stratigraphic profiles, and the same amount of

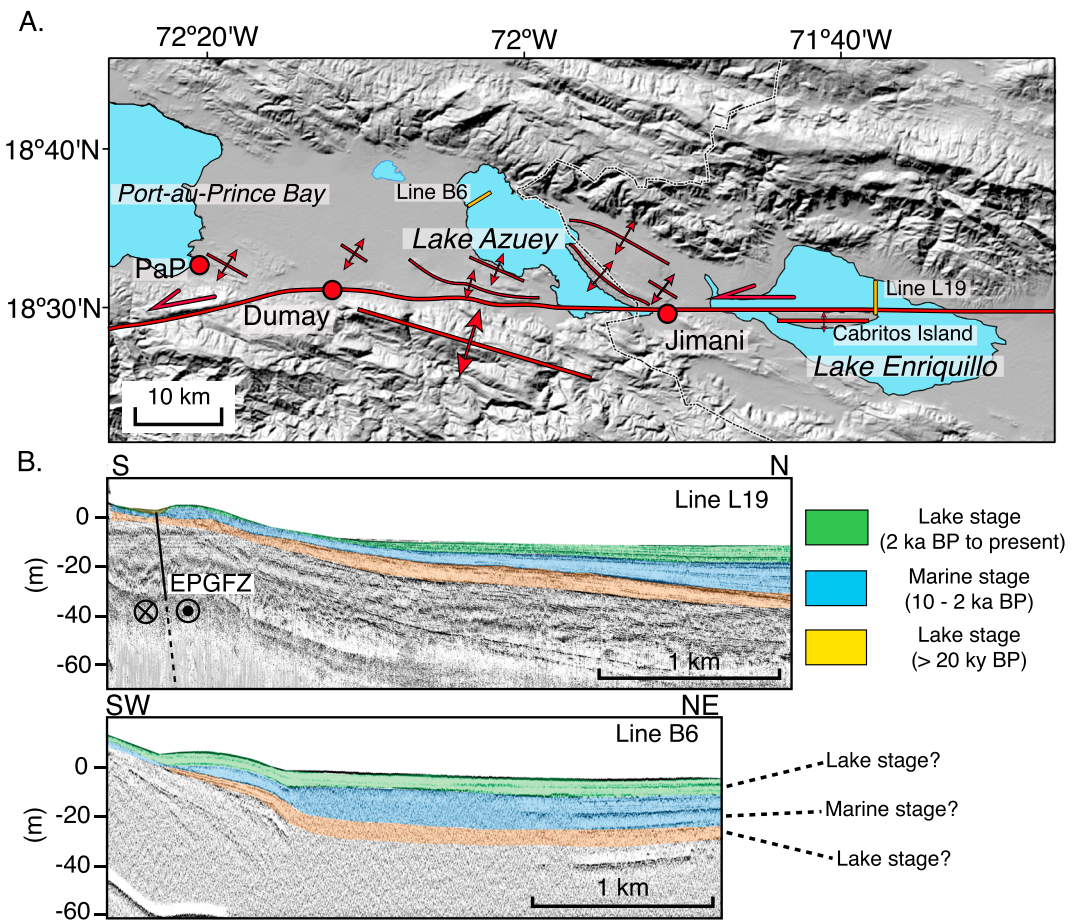


**Figure 6.** Structure of the EPGFZ in eastern Haiti and westernmost Dominican Republic. (a) Structural map of Lakes Azuey (surface 15-m ASL) and Lake Enriquillo (surface 46-m BSL) are presently separated by a shallow sill 30-m ASL in the isthmus near the town of Jimani. (b) Comparison of two Chirp lines from Lake Enriquillo by Rios et al., 2013 (2013, 3-km-long Line L19) and from our study of Lake Azuey (4-km-long Line B6). Chirp profiles from both lakes show similar sequences. Ages of units are known from Lake Enriquillo through both exposures around the subsea level lake and from lake coring by Rios et al. (2013). EPGFZ = Enriquillo-Plantain Garden fault zone.

sediment above the EPGFZ, it is reasonable to suggest that Lake Azuey and Lake Enriquillo share the similar sedimentation history as well as the same structural style and seismicity related to the EPGFZ and its oblique, thrust faults. However, this hypothesis remains speculative pending more coring in Lake Azuey.

The EPGFZ in both Lake Enriquillo and Lake Azuey is buried by 0.7 m of sediments. According to coring studies in the Dominican Republic (Rios et al., 2013; Taylor et al., 1985), the 5.2 m thickness of the latest lake stage (2 ka BP to present) gives a recent Holocene average sedimentation rate of 2.6 mm/year (Figure 6b). Using the average sediment rate, the most recent rupture of the EPGFZ would be dated to some 270 years ago. Given the historical earthquake records (Bakun et al., 2012), we suggest that the most recent rupture of the EPGFZ corresponds to the historical events of October or November 1751 (267 years ago) and that the deformed sediments in Lake Azuey are of Holocene age (Rios et al., 2013).

#### 4.5. Easternmost Extent of the EPGFZ Trace in Lake Enriquillo, Dominican Republic

Based on both of our lake surveys combined with a previous survey of Lake Enriquillo in the Dominican Republic (Rios et al., 2013) and the previous geologic mapping of the basinal and topographic correlation between the Cul-de-Sac basin in Haiti and the Enriquillo basin in the Dominican Republic (Mann et al., 1999, 1995), the basic question we pose is whether the EPGFZ extends as a continuous, strike-slip fault along the 120-km-long zone of deformation of Miocene and younger clastic rocks present between the two lakes (Figures 1b and 6a). Previous studies (Saint Fleur et al., 2015; Symithe & Calais, 2016) have proposed that the EPGFZ terminates as a strike-slip feature in the area south of Port-au-Prince. These studies further have proposed that transpressional

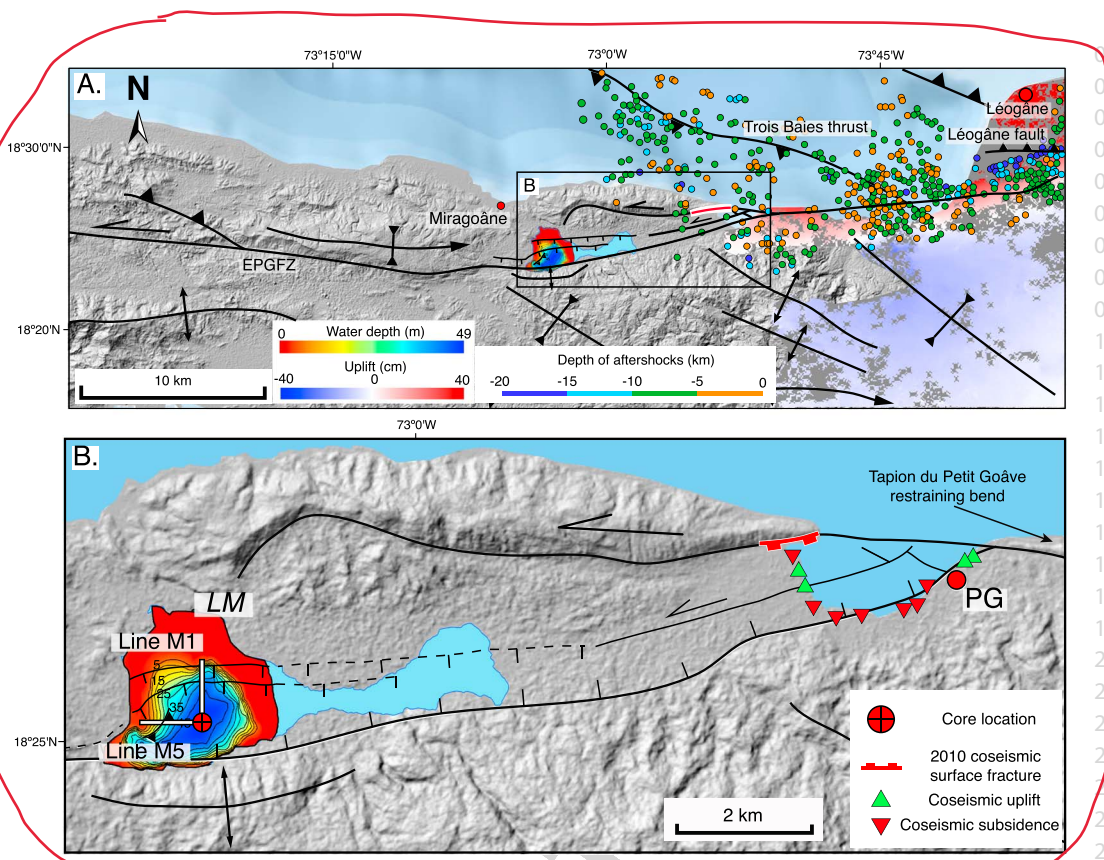


**Figure 7.** Structure and 2010 coseismic surface deformation of the western segments of the EPGFZ. (a) Fault map (Cowgill et al., 2012; Prentice et al., 2010) and map of 2010 aftershocks (Douilly et al., 2013) in Miragoâne-Léogâne region overlain with an InSAR image (courtesy of Eric Fielding at JPL; Hayes et al., 2010). (b) Zoom of the area of Petit Goâve and Lake Miragoâne showing the structure and bathymetry of the 14 km<sup>2</sup>, pull-apart basin underlying Lake Miragoâne during this study and details of the 2010 surface fracturing and coseismic subsidence in the Petit Goâve Bay (Hornbach et al., 2010; Prentice et al., 2010). LM = Lake Miragoâne; PG = Petit Goâve; EPGFZ = Enriquillo-Plantain Garden fault zone.

plate motion in the eastern Cul-de-Sac basin and the Enriquillo Valley in the Dominican Republic (Figures 1a and 6a) is entirely accommodated along the low-angle oblique-thrust structures that overthrust the southern edges of Lake Azuey and Lake Enriquillo.

A previous study of Lake Enriquillo by Rios et al. (2013) identified the break along the northeastern edge of Cabritos Island in Lake Enriquillo, which aligns exactly with the prominent, east-western lineament extending eastward from our map area in Lake Azuey (Figure 6a). The sonar results from both lakes show that the EPGFZ extends to at least to the eastern tip of Cabritos Island in the center of Lake Enriquillo, Dominican Republic (Figure 6a). This survey revealed a fault penetrating the youngest sediment layer of Holocene age which is consistent with recent activity on this segment of the EPGFZ (Figures 5a–5d). Therefore, we conclude that this linear, late Holocene strike-slip fault extends at 55 km (at least) to the eastern edge of Lake Enriquillo, where the previously documented (Mann et al., 1995) uplift of the Holocene reef fringes Lake Enriquillo.

## 5. Active Tectonics of the Area West of the 2010 Epicentral Zone in the Western Study Area: Léogâne Plain, Miragoâne Basin, and Their Adjacent Offshore Area

### 5.1. The Trois Baies Thrust Fault, Canal du Sud, as the Termination Structure for the 2010 Earthquake

The 2010 aftershock zone at the western and central parts of our study area (Figure 7a) reflects the rupture along the northwest striking, 20-km-long, submarine, Trois Baies thrust fault that forms the western extension of the 10- to 15-km-wide, transpressional zone north of the EPGFZ (Mercier de Lépinay et al., 2011). As the Trois Baies fault is a submarine fault, InSAR cannot be used to assess its 2010 coseismic similarity with folding and thrusting along the Léogâne thrust that affected the onshore, Léogâne plain (Figure 7a).

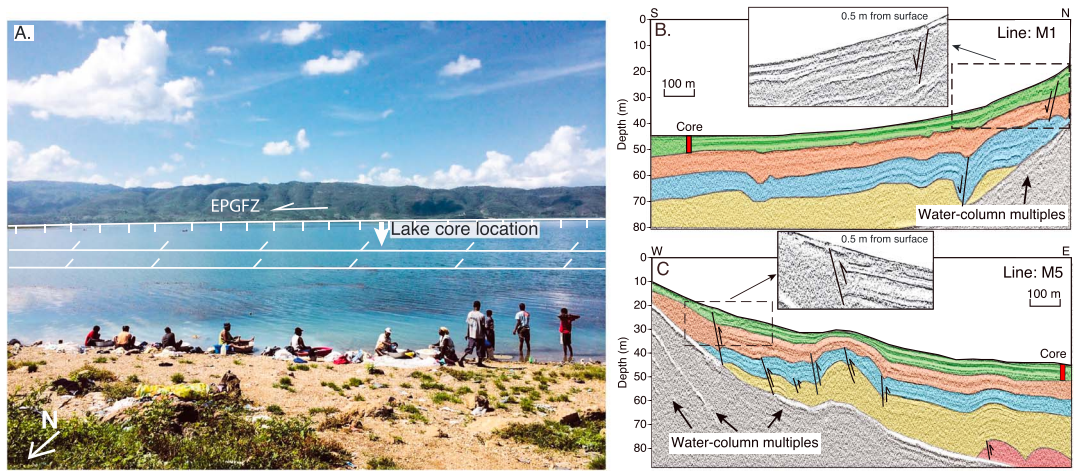


**Figure 8.** Geologic setting and sonar profiles from Lake Miragoâne. (a) View looking south across the 12-km-wide and 42.8-m-deep, freshwater lake. The 2-km-high ridge along the southern edge of the lake is the cumulative topographic scarp associated with the southernmost strand of the EPGFZ. The 7-m-long core was taken by Higuera-Gundy et al. (1999) but was not collected from the deepest part of the lake. (b) North-south trending line M1 (location shown in Figure 7b). (c) East-west trending line M5 (location shown in Figure 7b). In the lines shown in (b) and (c), the strands of the EPGFZ are both buried by 0.5 m of sediment. EPGFZ = Enriquillo-Plantain Garden fault zone.

Nevertheless, the same basic structural elements of the Léogâne plain are also observed for the offshore Trois Baies thrust fault, which include its proximity (1 km) to the EPGFZ and its steep ( $45^\circ$ ) but opposite (southwest) dip of the Trois Baies thrust fault (Figure 7). One of the most intense zones of 2010 coseismic, aftershock, coastal uplift (Hashimoto et al., 2011), and subsidence (Prentice et al., 2010) separates the oppositely dipping Léogâne and Trois Baies faults and may represent complex deformation at a transfer zone between the two, oppositely dipping thrust faults (Figures 7a and 7b). The aftershock study of the Trois Baies fault (Symithe & Calais, 2016) shows that its thrust character and oblique orientation in map view with the main EPGFZ is comparable to the cross sections of the eastern area in Figure 3. In the map view, the overall structure of this western part of the study area mirrors the same geometrical relationship between the oblique thrusts (such as the Trois Baies thrust fault) and the main EPGFZ as described at the eastern part of the study area (Figure 2).

## 5.2. Structure of the Miragoâne Pull-Apart Basin

In the onshore part of the western study area, Lake Miragoâne was interpreted as a 14-km<sup>2</sup> pull-part basin developed as a left-stepping, releasing bend on the EPGFZ paired with the adjacent Tapion du Petit Goâve restraining bend 12 km to the east (Figure 7; Cowgill et al., 2012; Mann et al., 1995). Bathymetry from our sonar data shows that the maximum water depth of Lake Miragoâne is 42.8 m (Figure 7b), which makes this lake the deepest (Higuera-Gundy et al., 1999) in the entire Caribbean region. The 30 m of recognizable stratigraphy (Figures 8b and 8c) from the sonar survey in Lake Miragoâne reveals a series of deformational features including major east-west normal faults, minor thrust faults at depth (some 20 m), and active folds at the lake bottom (Figure 8). The upper 7 m of the lake sediments were cored and dated at 10 ka at the bottom of the core (Higuera-Gundy et al., 1999). By applying the average sedimentary rate from the core data to the chirp sonar trace, we can extrapolate the sedimentation rate to the observed thickness of 30 m in the lake and estimate a minimum of 43 ka for the age of formation for the pull-apart basin along the EPGFZ. Core measurements of the E/P (evaporation and precipitation ratio from the  $\delta^{18}\text{O}$  of ostracod shells in the core sample) were carried out (Higuera-Gundy et al., 1999; Figure 9b). The core reveals that the uppermost part of the sediments is Holocene to the latest Pleistocene in age (Figure 9a). Pollen data from the core indicate alternating dry and wet environments.

## 5.3. Ages and Sedimentary Cycles of the Miragoâne Pull-Apart Basin

We applied a low-pass filter on the pollen log data (from the core acquired by Higuera-Gundy et al., 1999, in the center of the lake) and found a strong correlation between the pollen and sonar data (red curve in Figure 9b). To further investigate this interesting correlation between the paleoenvironmental and geophysical data, we use the filtered E/P log, considered as pseudoacoustic impedance log, to generate a synthetic sonar response (Figure 9b). The correlation suggests that the paleodepositional environment influences the

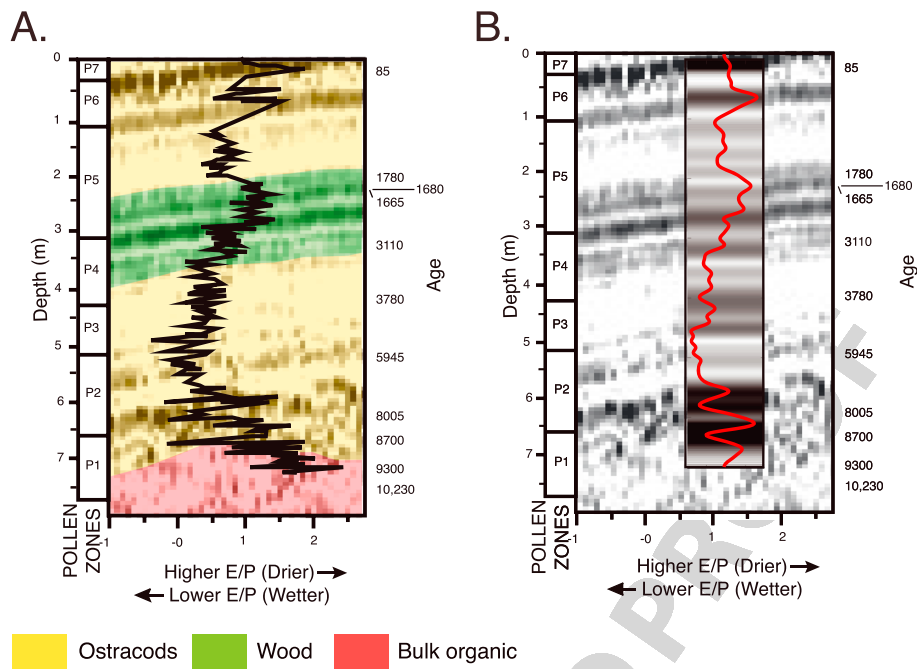


**Figure 9.** Core data from Lake Miragoâne. (a) Tie between chirp sonar and core with radiocarbon age control back to 10,230 years BP (Higuera-Gundy et al., 1999). Cyclicity is related to changes in lithology related to alternating wet and dry periods as shown. Yellow areas are shallow marine to freshwater, and green areas contain wood debris and may mark a period when the lake was dry. (b) Low-pass filtered E/P log (red) and the synthetic sonar profile generated from the low-pass filtered E/P log used as an acoustic impedance. The chirp sonar profiles are from the location of the red bar in the Figures 8b and 8c.

acoustic properties of the sediments, and sonar response may serve as a partial proxy for climatic processes with the sediment layers from drier climates (higher E/P) having stronger acoustic reflectivity and layers from wetter climates having weaker acoustic reflectivity. Combining the correlation between the pollen log and the acoustic reflections from the chirp sonar data, we can extend the sedimentary history of the upper 7 m from the log data to the entire sonar data set.

In the sonar profile, we find that the most recent rupture in the lake is buried by about 0.5-m sediment (Figures 8b and 8c). The core dating result from Higuera-Gundy et al. (1999) suggests the age of these rupture is about 300 years old. The historical document record (Bakun et al., 2012) indicates a historical earthquake that happened in this area in 1770 or 248 years ago. Considering the historical earthquake record (Bakun et al., 2012), the dating of the core, and the sonar interpretation in Lake Miragoâne all indicate that the most recent rupture in this lake is likely related to the historic earthquake of 1770 (Bakun et al., 2012).

## 6. Discussion

### 6.1. Proposed 3-D Structural Model for the 10- to 15-km-Wide Belt of Transpressional Deformation Along the Northern Edge of the EPGFZ

In summary, our lake studies, along with previous geologic and geophysical studies that we have compiled here, favor a model of a 10- to 15-km-wide transpressional zone that deforms thick, loosely consolidated, Miocene to recent clastic rocks in coastal, marine, and lake settings as shown schematically in our three-dimensional block diagram (Figure 10). Moving from Lake Azuey in the east to Lake Miragoâne in the west, the block diagram illustrates the along-strike alternations in the dips observed in the dips of the thrust faults that are oriented in an oblique and en echelon arrangement with the EPGFZ (Figure 10). EPGFZ. Fold axes north of the EPGFZ range from 3 to 20 km in length and are sigmoidal in trend with respect to the trace of the EPGFZ in map view (Figures 2a and 2b). Dip direction and amounts on these thrust faults vary from north dipping at 21° on the Jimani fault (Figures 5e and 10), south dipping on the Lamentin fault (Saint Fleur et al., 2015) at 40°, north dipping at 70° on the Léogâne fault active during the 2010 earthquake (A–A' in Figures 3 and 10), and south dipping on the Trois Baies fault at 45° (Figure 10).

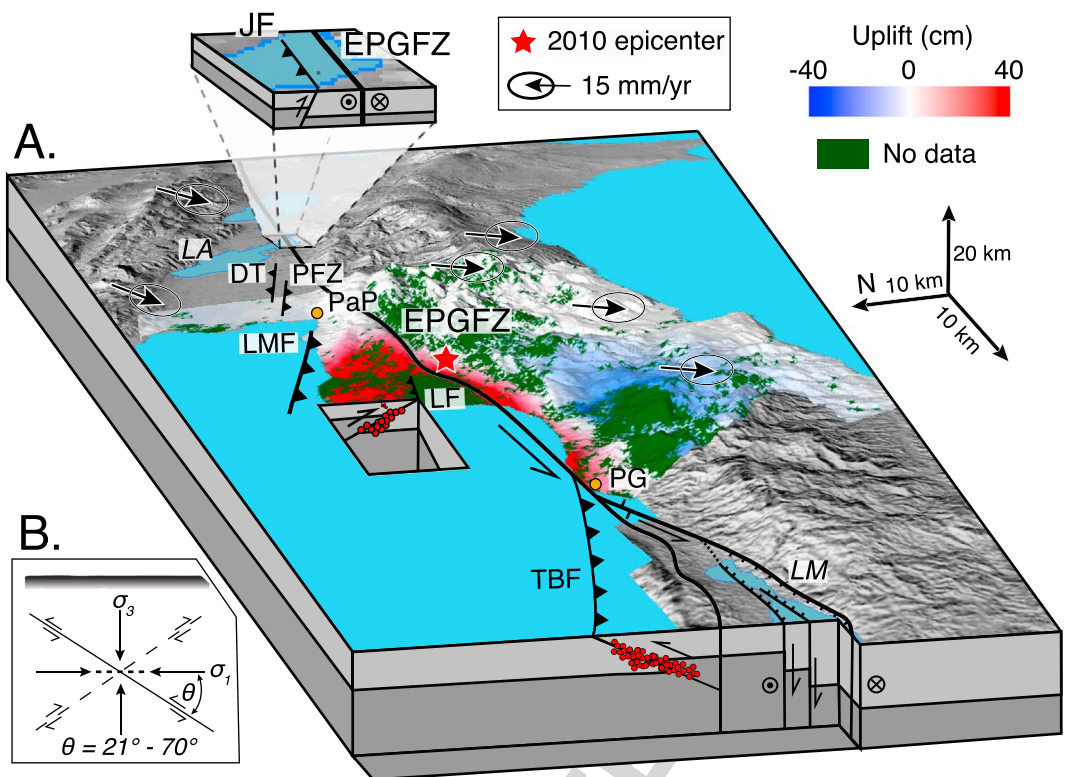


**Figure 10.** Schematic diagram of the conjugate thrust-fault model for the 10- to 15-km-wide belt of transpressional deformation along the northern edge of the EPGFZ. (a) Three-dimensional block diagram showing the structural aftershocks and the late Holocene strain partitioning in a 40-km-wide zone along a 120-km-long segment of the EPGFZ. Black arrows show the southwest direction of the GPS vectors relative to the Caribbean plate (Calais et al., 2010). The 2010 InSAR-derived surface deformation map (provided by Eric Fielding at JPL; Hayes et al., 2010) shows a large component of shortening accommodated on a 40-km-wide zone of oblique thrusts and folds to the west of the EPGFZ. Aftershock pattern shown in the cross section shows the northeastward dip of the *en echelon* thrusts adjacent to the EPGFZ uplifted the topographically lower basinal area to the north of the EPGFZ and depressed the mountainous area to the south of the EPGFZ. The alternating dip of the *en echelon* thrusts is related to their origin as conjugate thrust faults in a highly transpressional setting. PaP = Port-au-Prince; PG = Petit Goave; LA = Lake Azuey; LM = Lake Miragoâne-Léogâne; JF = Jimani thrust fault; DT = Dumay thrust; PFZ = Port-au-Prince fault zone; LMF = Lamartin thrust fault; TBF = Trois Baies thrust fault; LF = Léogâne fault; EPGFZ = Enriquillo-Plantain Garden fault zone. (b) Schematic diagram, modified from Sibson (2012), of the conjugate thrust faults.

South of the EPGFZ, transpressional folding in more rigid Cretaceous basalts and overlying Eocene limestone have broader folding wavelengths from 1 to 8 km and exhibit minor seismicity during and after the 2010 earthquake. In contrast, InSAR images of the 2010 earthquake indicate smaller folds and much more seismogenic deformation in the 10- to 15-km belt north of the EPGFZ. This deformational and seismogenic contrast north and south of the EPGFZ is likely related to rock type with weaker, poorly consolidated sedimentary rocks up to several kilometers north of the EPGFZ and stronger, more consolidated Paleocene limestone and Cretaceous basalt exposed in the highlands south of the EPGFZ (Mann et al., 1991; Figure 2).

We propose that the folds north of the EPGFZ formed originally as conjugate thrust faults within a highly transpressional, tectonic setting indicated by GPS vectors (Calais et al., 2010). Conjugate thrust faults are common in thick, clastic sedimentary basins undergoing active, subhorizontal shortening (Sibson, 2012), as documented in the  $M_w$  7.6 Chi-Chi Taiwan earthquake in 1999 (Chen et al., 2002) or the  $M_w$  7.1 Kumamoto Japan earthquake in 2016 (Lin & Chiba, 2017). Aftershocks north of the EPGFZ reflect the most recent phase of NE-SW shortening on the 70° dipping, conjugate reverse fault planes (Nettles & Hjörleifsdóttir, 2010), of the deeply buried Léogâne thrust fault, as shown in the cross-section of A–A' in Figure 3.

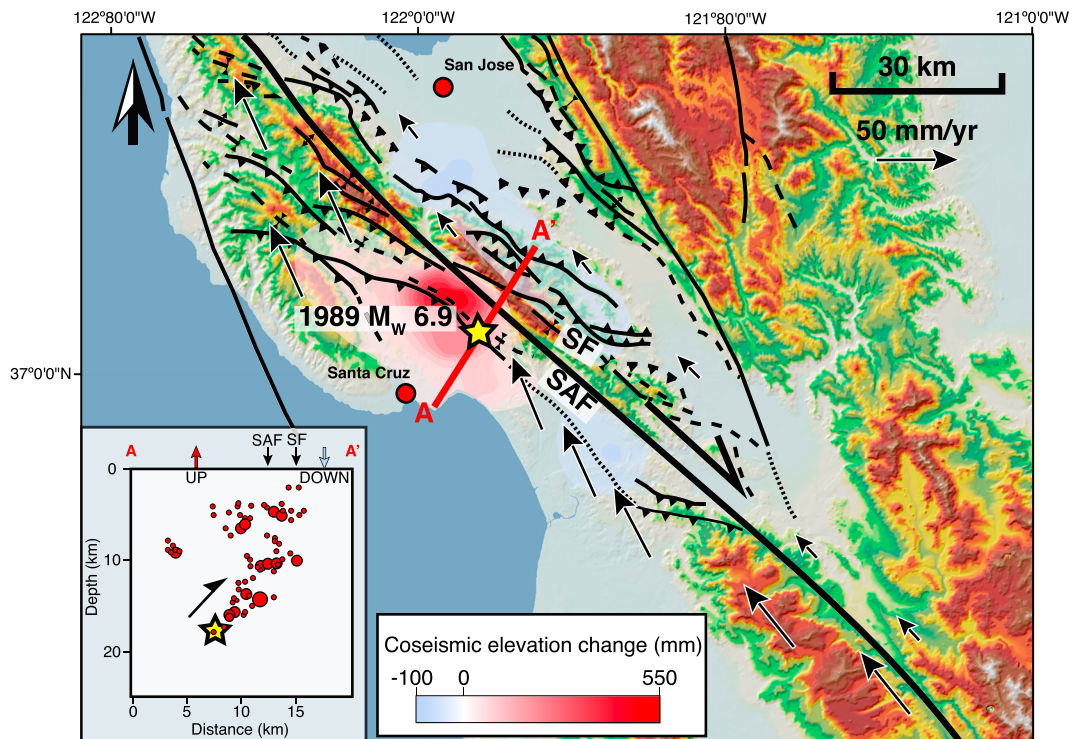


**Figure 11.** Structural map of the southern San Francisco Bay region, the coseismic elevation, and the aftershock cross section of 1989  $M_w$  6.9 Loma Prieta earthquake. The selected GPS vectors relative to a fixed North America plate are from University Navstar Consortium (2009). The coseismic elevation change and aftershock cross section are modified from Marshall et al. (1991). SAF = San Andreas Fault; SF = Sargent Fault. Aftershock pattern in the cross section shows that the southwest dip of the **en echelon** thrust adjacent to the San Andreas fault uplifted the topographically lower basinal area and depressed the mountainous area to the northeast of the San Andreas fault.

## 6.2. Analogy Between the 2010 Coseismic Transpressional Deformation in Haiti and the 1989 Loma Prieta Earthquake in Northern California

A similar pattern of transpression in a restraining bend setting to Haiti has been described for 1989  $M_w$  6.9 Loma Prieta earthquake (Marshall et al., 1991; Figure 11). The selected GPS vectors relative to a fixed North America plate (University Navstar Consortium, 2009) indicate the transpressional setting within a gentle restraining bend setting. In the inset map of Figure 11, the 1989 hypocentral area maps of aftershocks (Marshall et al., 1991) reveal the steep (~61°) dip of oblique reverse faults of the collective Sargent and San Andreas faults. As observed during the 1989 earthquake, the southwestward dip of the en echelon reverse faults produced coseismic uplift up to 0.55 m of the lowland areas southwest of the San Andrea fault and depression by up to 0.1 m of the mountainous area to the northeast of the San Andreas fault (Marshall et al., 1991). The thrusting was blind with the  $M_w$  7.1 earthquake not being accompanied by coseismic, surface breaks. The pattern of aftershocks (seen on the cross section in Figure 11) suggests a conjugate pair of reverse faults with the dominant motion on the south dipping fault plane, similar to the conjugate pair seen on the cross section of the Léogâne fault as defined by its 2010 aftershocks (cross-section A–A' in Figure 3).

As in the 2010  $M_w$  7.0 Haiti earthquake on the previously unknown Léogâne thrust, a secondary, blind thrust fault (Olson, 1990) beneath the surface trace of the Sargent fault, and oblique to the main San Andreas strike-slip fault (shown in inset map of Figure 11), played a major role in the 1989 fault rupture and resulting pattern of regional uplift shown in red color to the southwest and regional subsidence shown in blue color to the northeast (Figure 11).

While the oblique and en echelon thrust planes form smaller fault segments ranging in length from 3 to 11 km (Figure 2a), the 2010 Haiti earthquake demonstrates that oblique thrusts like the Léogâne fault are capable of producing a  $M_w$  7.0 earthquake with devastating results, especially when coupled with inadequate construction practices (Symithe & Calais, 2016). Paleoseismic estimates of the age of the most recent deformation of Lake Azuey, eastern Haiti, suggest that the latest activity of the EPGFZ in this area was in 1751

(Bakun et al., 2012; Prentice et al., 2010). Similar analysis indicates that the latest earthquake event in the Lake Miragoâne area, western Haiti, was in 1770 (Bakun et al., 2012). Bakun et al. (2012) conclude that the earthquake recurrence cycle along the EPGFZ is about 250 years. Therefore, in the highly transpressional setting of Hispaniola, the earthquake cycle may consist of a complex alternation between ruptures on the EPGFZ and ruptures on the oblique, en echelon thrusts and related folds.

The 2010  $M_w$  7.0 earthquake released part of a century-long accumulation of stress in the region but as the oblique thrusts may not be directly linked to the EPGFZ, it is likely that stresses on the EPGFZ have continued to accumulate since the eighteenth century (Prentice et al., 2010). Integrated paleoseismic study of the EPGFZ with the commonly buried, oblique thrust faults, using geophysical and geologic methods, can help to inform the critical social issue of how future earthquakes will be partitioned between the larger EPGFZ and other more obscure, oblique faults.

## 7. Conclusions

The main conclusions of the study are as follows:

1. High-resolution sonar data from two Haitian Lakes that completely straddle the EPGFZ and its northern flank demonstrate the presence of a 10- to 15-km-wide, 120 km-long, late Holocene, fold-and-thrust belt, which is deforming both the clastic lowland basins along the northern edge of the EPGFZ and the steep topographic highlands to the south.
2. In the eastern part of the study area, sonar results from Lake Azuey show that the 250- to 500-m-wide EPGFZ is more deeply buried and less active than the adjacent, newly discovered, northwest striking, north-east dipping Jimani thrust fault. This structural relationship between the more deeply buried EPGFZ and more active Jimani thrust fault in Lake Azuey is identical to the epicentral area of the 2010 Haiti earthquake 70 km to the west: the 2010 seismogenic, Léogâne blind thrust fault is northwest-to-east striking, and the quiescent fault to the south during the 2010 earthquake is the east-west striking, subvertical EPGFZ.
3. The geographic distribution of 2010 aftershocks revealed that the seismogenic motions of the Léogâne thrust fault and smaller motions on the EPGFZ terminated on a similar northwest striking fault: the submarine Trois Baies thrust fault. In the westernmost part of the study area, sonar results from Lake Mirogoâne show two overlapping and active strands of the EPGFZ and were instead diverted onto the Trois Baies thrust fault.
4. Our survey confirmed the pull-apart origin of Lake Mirogoâne and the lack of deformation on this western segment of the EPGFZ during the 2010  $M_w$  7.0 earthquake. Integration of the geologic data across the study area shows an alternation in dip along nine northwest striking, thrust faults at spacing of 5 to 40 km.
5. We interpret this 10- to 15-km-wide belt of late Holocene deformation in clastic basins north of the EPGFZ, with Cul-de-Sac intermontane basin in the east and the low-relief coastal plain along Port-au-Prince bay and the Canal du Sud to the west, as the accommodation of transpressional strain supported by highly oblique GPS vectors across the study area. In this transpressional zone, coseismic deformation alternates at recurrence intervals of centuries between oblique shortening structures, such as Léogâne thrusts, Jimani thrusts, and Trois Baies thrusts, and strike-slip ruptures along the narrow and well-defined main trace of the EPGFZ.
6. The presence of en echelon thrust faults north of the EPGFZ with spacings of 1–8 km and alternating dips is proposed to have formed as a conjugate thrust and reverse faults. The Léogâne thrust dips to the north along with the newly described Jimani thrust fault dip northeast, while other faults like the Trois Baies and Lamartin thrust faults dip to the southwest.
7. Our results, including the eastward extension of the EPGFZ into Dominican Republic, support the *thick-skinned* strike-slip model along a 10- to 15-km-wide corridor of left-lateral shearing centered on the EPGFZ as opposed to the southwestward propagation of the Trans-Haitian fold-and-thrust belt proposed by Pubellier et al. (2000).

## References

-  Sun, W. H., Flores, C. H., & Uri, S. (2012). Significant earthquakes on the Enriquillo fault system, Hispaniola, 1500–2010: Implications for seismic hazard. *Bulletin of the Seismological Society of America*, 102(1), 18–30.
- Benford, B., DeMets, C., & Calais, E. (2012). GPS estimates of microplate motions, northern Caribbean: Evidence for a Hispaniola microplate and implications for earthquake hazard. *Geophysical Journal International*, 191(2), 481–490.

- Bien-Aimé Momplaisir, R. (1986). Contribution à l'étude géologique de la partie orientale du Massif de la Hotte (Presqu'île du Sud d'Haïti): Synthèse structurale des marges de la presqu'île à partir de données sismiques (PhD Thesis), Université Pierre et Marie Curie (Paris VI), Paris.
- Bilham, R. (2010). Lessons from the Haiti earthquake. *Nature*, 463(7283), 878–879.
- Bilham, R., & Fielding, E. (2013). Remote sensing and the search for surface rupture, Haiti 2010. *Natural Hazards*, 68(1), 213–217.
- Bourgueil, B., Andrieuff, P., Lasnier, J., Gonnard, R., Le Metour, J., & Rancon, J.-P. (1988). Synthèse géologique De La République D'Haïti, Technical Report, Bureau Des Mines Et De L'Energie. Haïti Port-au-Prince.
-  Grufa, J. G., Ten Brink, U. S., Carbó-Gorosabel, A., Muñoz-Martín, A., & Ballesteros, M. G. (2009). Morphotectonics of the central Muertos thrust belt and Muertos Trough (northeastern Caribbean). *Marine Geology*, 263(1), 7–33.
- Calais, E., Freed, A., Mattioli, G., Amelung, F., Jónsson, S., Jansma, P., et al. (2010). Transpressional rupture of an unmapped fault during the 2010 Haiti earthquake. *Nature Geoscience*, 3(11), 794–799.
- Calais, E., Mazabraud, Y., Mercier de Lépinay, B., Mann, P., Mattioli, G., & Jansma, P. (2002). Strain partitioning and fault slip rates in the northeastern Caribbean from GPS measurements. *Geophysical Research Letters*, 29(18), 1856. <https://doi.org/10.1029/2002GL015397>
- Calais, É., Symithe, S., de Lépinay, B. M., & Prépetit, C. (2016). Plate boundary segmentation in the northeastern Caribbean from geodetic measurements and Neogene geological observations. *Comptes Rendus Geoscience*, 348(1), 42–51.
- Chen, K.-C., Huang, B.-S., Wang, J.-H., & Yen, H.-Y. (2002). Conjugate thrust faulting associated with the 1999 Chi-Chi, Taiwan, earthquake sequence. *Geophysical Research Letters*, 29(8), 1277. <https://doi.org/10.1029/2001GL014250>
- Corbeau, J., Rolandone, F., Leroy, S., Meyer, B., Mercier de Lépinay, B., Ellouz-Zimmermann, N., & Momplaisir, R. (2016). How transpressive is the northern Caribbean plate boundary? *Tectonics*, 35, 1032–1046. <https://doi.org/10.1002/2015TC003996>
- Cowgill, E., Bernardin, T. S., Oskin, M. E., Bowles, C., Yikilmaz, M. B., Kreylos, O., et al. (2012). Morelan Interactive terrain visualization enables virtual field work during rapid scientific response to the 2010 Haiti earthquake. *Geosphere*, 8(4), 787–804.
- Cox, B. R., Bachhuber, J., Rathje, E., Wood, C. M., Dulberg, R., Kottke, A., et al. (2011). Shear wave velocity-and geology-based seismic microzonation of Port-au-Prince, Haïti. *Earthquake Spectra*, 27(S1), S67–S92.
- Dolan, J. F., Mullins, H. T., & Wald, D. J. (1998). Active tectonics of the north-central Caribbean: Oblique collision, strain partitioning, and opposing subducted slabs. *Special Papers-Geological Society of America*, 326, 1–62.
- Douilly, R., Aochi, H., Calais, E., & Freed, A. (2015). Three-dimensional dynamic rupture simulations across interacting faults: The Mw 7.0, 2010, Haïti earthquake. *Journal of Geophysical Research: Solid Earth*, 120, 1108–1128. <https://doi.org/10.1002/2014JB011595>
- Douilly, R., Haase, J. S., Ellsworth, W. L., Bouquin, M.-P., Calais, E., Symithe, S. J., et al. (2013). Crustal structure and fault geometry of the 2010 Haïti earthquake from temporary seismometer deployments. *Bulletin of the Seismological Society of America*, 103(4), 2305–2325.
- Fielding, E. J., Sladen, A., Li, Z., Avouac, J.-P., Bürgmann, R., & Ryder, I. (2013). Kinematic fault slip evolution source models of the 2008 M7.9 Wenchuan earthquake in China from SAR interferometry, GPS and teleseismic analysis and implications for Longmen Shan tectonics. *Geophysical Journal International*, 194(2), 1138–1166. <https://doi.org/10.1093/gji/ggt155>
- Frankel, A., Harmsen, S., Mueller, C., Calais, E., & Haase, J. (2011). Seismic hazard maps for Haïti. *Earthquake Spectra*, 27(S1), S23–S41.
- Greer, L., & Swart, P. K. (2006). Decadal cyclicity of regional mid-Holocene precipitation: Evidence from Dominican coral proxies. *Paleoceanography*, 21, PA2020. <https://doi.org/10.1029/2005PA001166>
- Grindlay, N. R., Hearne, M., & Mann, P. (2005). High risk of tsunami in the northern Caribbean, Eos. *Transactions American Geophysical Union*, 86(12), 121–126.
- Hashimoto, M., Fukushima, Y., & Fukahata, Y. (2011). Fan-delta uplift and mountain subsidence during the Haïti 2010 earthquake. *Nature Geoscience*, 4(4), 255–259.
- Hayes, G., Briggs, R., Sladen, A., Fielding, E., Prentice, C., Hudnut, K., et al. (2010). Complex rupture during the 12 January 2010 Haïti earthquake. *Nature Geoscience*, 3(11), 800–805.
- Higuera-Gundy, A., Brenner, M., Hodell, D. A., Curtis, J. H., Leyden, B. W., & Binford, M. W. (1999). A 10,300 14 C yr record of climate and vegetation change from Haïti. *Quaternary Research*, 52(2), 159–170.
- Hornbach, M. J., Braudy, N., Briggs, R. W., Cormier, M.-H., Davis, M. B., Diebold, J. B., et al. (2010). High tsunami frequency as a result of combined strike-slip faulting and coastal landslides. *Nature Geoscience*, 3(11), 783–788.
- Kocel, E., Stewart, R. R., Mann, P., & Chang, L. (2016). Near-surface geophysical investigation of the 2010 Haïti earthquake epicentral area: Léogâne, Haïti. *Interpretation*, 4(1), T49–T61.
- Koehler, R., & Mann, P. (2011). Field observations from the January 12, 2010, Haïti earthquake: Implications for seismic hazards and future post-earthquake reconnaissance investigations in Alaska. *Report of Investigations*, 2, 24.
- Kroehler, M. E., Mann, P., Escalona, A., & Christeson, G. L. (2011). Late Cretaceous-Miocene diachronous onset of back thrusting along the South Caribbean deformed belt and its importance for understanding processes of arc collision and crustal growth. *Tectonics*, 30, TC6003. <https://doi.org/10.1029/2011TC002918>
- Lin, A., & Chiba, T. (2017). Coseismic conjugate faulting structures produced by the 2016 Mw 7.1 Kumamoto earthquake, Japan. *Journal of Structural Geology*, 99, 20–30.
- Mann, P. (1999). Caribbean sedimentary basins: Classification and tectonic setting from Jurassic to present. *Sedimentary Basins of the World*, 4, 3–31.
- Mann, P., Calais, E., Ruegg, J.-C., DeMets, C., Jansma, P. E., & Mattioli, G. S. (2002). Oblique collision in the northeastern Caribbean from GPS measurements and geological observations. *Tectonics*, 21(6), 1057. <https://doi.org/10.1029/2001TC001304>
- Mann, P., Draper, G., Lewis, J. F., et al. (1991). An overview of the geologic and tectonic development of Hispaniola, Geologic and tectonic development of the North America-Caribbean plate boundary in Hispaniola. *Geological Society of America Special Paper*, 262, 1–28.
- Mann, P., Taylor, F., Edwards, R. L., & Ku, T.-L. (1995). Actively evolving microplate formation by oblique collision and sideways motion along strike-slip faults: An example from the northeastern Caribbean plate margin. *Tectonophysics*, 246(1), 1–69.
- Marshall, G. A., Stein, R. S., & Thatcher, W. (1991). Faulting geometry and slip from co-seismic elevation changes: The 18 October 1989, Loma Prieta, California, earthquake. *Bulletin of the Seismological Society of America*, 81(5), 1660–1693.
- Massoni, P. (1955). Haïti: reine des Antilles. Nouvelles Éditions Latines.**
- McHugh, C. M., Seeber, L., Braudy, N., Cormier, M.-H., Davis, M. B., Diebold, J. B., et al. (2011). Offshore sedimentary effects of the 12 January 2010 Haïti earthquake. *Geology*, 39(8), 723–726.
- Medley, P., Tibert, N. E., Patterson, W. P., Curran, H. A., Greer, L., & Colin, J.-P. (2007). Paleosalinity history of middle Holocene lagoonal and lacustrine deposits in the Enriquillo Valley, Dominican Republic based on pore morphometrics and isotope geochemistry of Ostracoda. *Micropaleontology*, 53(5), 409–419.
- Mercier de Lépinay, B., Deschamps, A., Klingelhofer, F., Mazabraud, Y., Delouis, B., Clouard, V., et al. (2011). The 2010 Haïti earthquake: A complex fault pattern constrained by seismologic and tectonic observations. *Geophysical Research Letters*, 38, L22305. <https://doi.org/10.1029/2011GL049799>

- Moknatian, M., Piasecki, M., & Gonzalez, J. (2017). Development of geospatial and temporal characteristics for Hispaniola's Lake Azuei and Enriquillo using Landsat imagery. *Remote Sensing*, 9(6), 510.
- Mount, V. S., & Suppe, J. (1987). State of stress near the San Andreas fault: Implications for wrench tectonics. *Geology*, 15(12), 1143–1146.
- Nettles, M., & Hjörleifsdóttir, V. (2010). Earthquake source parameters for the 2010 January Haiti main shock and aftershock sequence. *Geophysical Journal International*, 183(1), 375–380.
- Odonne, F., & Vialon, P. (1983). Analogue models of folds above a wrench fault. *Tectonophysics*, 99(1), 31–46.
- Olson, J. A. (1990). Seismicity in the twenty years preceding the Loma Prieta California earthquake. *Geophysical Research Letters*, 17(9), 1429–1432.
- Paultre, P., Calais, É., Proulx, J., Prépetit, C., & Ambroise, S. (2013). Damage to engineered structures during the 12 January 2010, Haiti (Léogâne) earthquake. *Canadian Journal of Civil Engineering*, 40(8), 777–790.
- Piasecki, M., Moknatian, M., Moshary, F., Cleto, J., Leon, Y., Gonzalez, J., & Comarazamy, D. (2016). Report: Bathymetric survey for Lakes Azuei and Enriquillo Hispaniola. Tech. Rep.: City University of New York (CUNY).
- Prentice, C., Mann, P., Crone, A., Gold, R., Hudnut, K., Briggs, R., et al. (2010). Seismic hazard of the Enriquillo-Plantain Garden fault in Haiti inferred from palaeoseismology. *Nature Geoscience*, 3(11), 789–793.
- Prentice, C. S., Mann, P., Peña, L. R., & Burr, G. (2003). Slip rate and earthquake recurrence along the central Septentrional fault, North American–Caribbean plate boundary, Dominican Republic. *Journal of Geophysical Research*, 108(B3), 2149. <https://doi.org/10.1029/2001JB000442>
- Prentice, C. S., Mann, P., Taylor, F., Burr, G., & Valastro, S. (1993). Paleoseismicity of the North American–Caribbean plate boundary (Septentrional fault), Dominican Republic. *Geology*, 21(1), 49–52.
- Pubellier, M., Mauffret, A., Leroy, S., Vila, J. M., & Amilcar, H. (2000). Plate boundary readjustment in oblique convergence: Example of the Neogene of Hispaniola, Greater Antilles. *Tectonics*, 19(4), 630–648.
- Rathje, E., Bachhuber, J., Cox, B., French, J., Green, R., Olson, S., et al. (2014). Geotechnical reconnaissance of the 2010 Haiti Earthquake: GEER. (Geotechnical Extreme Events Reconnaissance).
- Rico, P. (2017). Hydrodynamic study of Lake Enriquillo in Dominican Republic. *Journal of Geoscience and Environment Protection*, 5, 115–124.
- Rios, J., McHugh, C., Hornbach, M., Mann, P., Wright, V., & Gurung, D. (2013). Holocene activity of the Enriquillo-Plantain Garden Fault in Lake Enriquillo derived from seismic stratigraphy. *AGU Fall Meeting Abstracts*, 1, 2629.
- Romero Luna, E. J., & Poteau, D. (2011). Water level fluctuations of Lake Enriquillo and Lake Saumatre in response to environmental changes: Cornell University.
- Saint Fleur, N., Feuillet, N., Grandin, R., Jacques, E., Weil-Accardo, J., & Klinger, Y. (2015). Seismotectonics of southern Haiti: A new faulting model for the 12 January 2010 M7.0 earthquake. *Geophysical Research Letters*, 42, 10,273–10,281. <https://doi.org/10.1002/2015GL065505>
- Schwartz, A. (1980). The herpetogeography of Hispaniola, West Indies. *Studies on the fauna of Curaçao and other Caribbean Islands*, 61(189), 86–127.
- Segall, P., & Lisowski, M. (1990). Surface displacements in the 1906 San Francisco and 1989 Loma Prieta earthquakes. *Science*, 250(4985), 1241–1244.
- Sibson, R. (2012). Reverse fault rupturing: Competition between non-optimal and optimal fault orientations. *Geological Society, London, Special Publications*, 367(1), 39–50.
- Sylvester, A. G. (1988). Strike-slip faults. *Geological Society of America Bulletin*, 100(11), 1666–1703.
- Symithe, S., & Calais, E. (2016). Present-day shortening in Southern Haiti from GPS measurements and implications for seismic hazard. *Tectonophysics*, 679, 117–124.
- Symithe, S. J., Calais, E., Haase, J. S., Freed, A. M., & Douilly, R. (2013). Coseismic slip distribution of the 2010 M 7.0 Haiti earthquake and resulting stress changes on regional faults. *Bulletin of the Seismological Society of America*, 103(4), 2326–2343.
- Taylor, F., Mann, P., Valastro, Jr. S., & Burke, K. (1985). Stratigraphy and radiocarbon chronology of a subaerially exposed Holocene coral reef, Dominican Republic. *The Journal of Geology*, 93(3), 311–332.
- Terrier, M., Bialkowski, A., Nachbaur, A., Prépetit, C., & Joseph, Y. (2014). Revision of the geological context of the Port-au-Prince metropolitan area, Haiti: Implications for slope failures and seismic hazard assessment. *Natural Hazards and Earth System Sciences*, 14(9), 2577–2587.
- University Navstar Consortium (2009). PBO GPS velocities in southern California.
- Wang, J., & Stewart, R. (2015). Inferring marine sediment type using chirp sonar data: Atlantis Field, Gulf of Mexico. In *2015 SEG Annual Meeting*, Society of Exploration Geophysicists, New Orleans, Louisiana.
- Wright, V. D., Hornbach, M. J., McHugh, C., & Mann, P. (2015). Factors contributing to the 2005-present, rapid rise in lake levels, Dominican Republic and Haiti (Hispaniola). *Natural Resources*, 6(8), 465–481.